Partial Combustion of Fuel Oil with Oxygen and Application to Smelting Iron Ore

by Jerome Feinman and
David A. Muskat*

Applied Research Laboratory
United States Steel Corporation
Monroeville, Pennsylvania

Much interest in alternative smelting processes based on cheaper fuels than metallurgical coke has developed during the past decade. Many processes have been developed, however, none of these processes have proven competitive with the blast furnace in the United States. In this context, it was decided to study a proposed smelting process in which all the reducing gases and heat for smelting come from the partial combustion of fuel oil and/or pulverized coal with oxygen at the bottom of a shaft reactor. Some anticipated advantages of such a process over the blast furnace are elimination of the stoves and associated equipment for heating the blast, reduction or elimination of coke requirements, and production of hot metal at much higher rates than are presently obtained with blast furnaces.

Preliminary heat and material balances indicated that the proposed process is feasible. Several important factors associated with the operation of a partial-combustion burner and with the operation of the reactor, however, could not be investigated theoretically. With respect to burner operation, the extent of conversion of fuel oil with oxygen to CO and H_2, the nature of any solid carbon formed during partial combustion, and the stability of combustion were the most important factors to be determined experimentally. As for the operation of the reactor, it was not known whether smooth flow of materials and effective contact between gases and solids could be achieved without the leavening action provided by coke in the blast furnace. In addition, it was not known whether sufficient residence time can be obtained to complete reduction at the high throughput rates assumed in the theoretical analysis.

Theoretical and Practical Considerations

Figure 1 shows that the theoretical flame temperature for stoichiometric partial combustion of No. 6 fuel oil with oxygen to produce CO and H_2 is 3375 F. With 10 percent excess oxygen, the flame temperature would be approximately 4000 F. If 10 percent ungasified carbon were formed with stoichiometric oxygen, the flame temperature would be approximately 3700 F. Thus, the required temperatures for smelting iron oxide are theoretically attainable. Whether they could be obtained in practice, however, remained to be determined.

* Present address - Lubrizol Company, Painesville, Ohio

In most commercial applications, combustion refers to the rapid oxidation of a material with the evolution of large quantities of heat. Usually, the specific rates of the chemical reactions occurring in the combustion process are so rapid that physical transport phenomena control the rate of combustion. These physical characteristics are directly related to the degree of mixing of the reactants. A device known as a burner is used to prepare and introduce the reactants into the reaction zone in such a manner as to produce an efficient rate of combustion.

The most effective burner for high-intensity combustion would mix the fuel with the oxygen before introduction into the combustion chamber. Many gas burners premix all or most of the air or oxygen needed for combustion with the gas and produce a high-temperature flame. A bunsen burner premixes only as much air as can be aspirated; its flame is therefore not as hot nor as well defined as the flame of burners utilizing completely premixed air and fuel because some of the air needed for combustion must come from the surroundings of the flame. When all aspirated air to the burner is shut off, the flame becomes long and poorly defined because all the air must mix with the gas by diffusional means, a much slower method of mixing.

Because liquid fuels cannot be appreciably premixed before burning, the rate of combustion is controlled by the mixing in the combustion zone. To facilitate combustion, liquid fuels are usually injected into the combustion zone through an atomizing nozzle. There are three types of atomizers: (1) pneumatic nozzles that use air, steam, or some other gas to atomize the liquid; (2) high-pressure nozzles that force the liquid through a small orifice; and (3) mechanical devices that use rotating discs to break up the liquid. The energy used to atomize the liquid is greatest for the first type, which usually produces a spray of finer droplets than the other types.

There are two common methods for providing good mixing of the reactants in the combustion zone. The first is direct impingement of the fuel and air jets, each introduced into the combustion zone at different angles. In the second method, opposite radial velocity components are imparted to the two streams by the use of vanes in each injector tube. For efficient operation, most burners are designed to use one of these methods.

Liquid fuels such as fuel oil burn according to the following simplified mechanisms:

1. The volatile components in the oil are vaporized
2. The vapors react with oxygen, evolving sufficient heat to propagate the combustion. If sufficient oxygen is not immediately available to react with all the carbon in the vaporized portion of the fuel, the unreacted hydrocarbons will crack to form solid carbon particles and hydrogen.

3. The nonvolatile matter (primarily solid carbon) is burned. This carbon, as well as any carbon formed by the cracking of hydrocarbons, is consumed by a relatively slow solid-gas reaction mechanism.

Previous workers have found that the reaction time of the solid residue is as much as 10 times that of the volatile matter.[1,2]* These experiments were performed in an atmosphere containing an excess of oxygen. The increase in burning time for cases in which there is a deficiency of oxygen, such as in a partial-combustion process, would probably be even greater. It is therefore desirable to minimize the amount of solid carbon formed during primary combustion. The minimum solid carbon would be comprised of oil residue, with none being formed by cracking of volatiles.

When atomization is good, the rates of evaporation of volatiles and reaction of volatiles with oxygen are very rapid. Therefore, to prevent any of the volatiles from cracking, oxygen must be made available before the hydrocarbon vapors reach the cracking temperature. Because the oxygen and oil are not premixed, very rapid mixing must occur as soon as these reactants enter the combustion chamber. Because this mixing can only occur by eddy and molecular diffusion, it is evident that mixing is normally the limiting factor in establishing the rate of combustion. This conclusion is based on work done under conditions of complete combustion, and is probably even more restrictive under conditions of partial combustion.

Description of Burner System and Operating Procedure

In view of the theoretical and practical considerations, it was apparent that the combustion chamber would have to be constructed of a refractory capable of withstanding very high temperatures in both oxidizing and reducing atmospheres. It was also apparent that because of the small volume of oxygen needed per unit of fuel compared with a complete combustion burner operating on air — only 1/16 the volume of reacting gas and 1/3 the oxygen is required for partial combustion using oxygen — satisfactory mixing of the reactants would be considerably more difficult. If sufficient mixing were not provided, flame stability would decrease, localized excessive temperatures would result, and large quantities of solid carbon would be formed that would greatly increase the time needed to complete the gasification process; additional combustion-chamber volume would be needed to produce a given amount of reducing gas.

These factors were considered in selecting a commercial fuel-oil burner that was adaptable for use as a partial-combustion burner. An air-atomizing vortex burner was procured that fulfilled these requirements. In addition to the fine atomization obtainable with this burner, the main oxygen stream had a counterclockwise motion imparted to it by

*See References

means of vanes in the windbox. This arrangement provided one of the most efficient means available in a commercial burner for mixing the fuel oil and oxygen.

Figure 2 shows details of the oil-injection nozzle, the center cone, the windbox vane detail and the oxygen nozzle comprising the essential parts of the burner, Figure 3 is a section view of the assembled burner, and Figure 4 is a section view of the atmospheric test chamber.

Figure 5 shows a schematic piping diagram for the burners. The oil rate is obtained by measuring the change in weight of the oil-supply barrel with time. A positive-displacement pump transports the oil against a constant delivery pressure maintained by the pressure-regulating valve. The oil rate is controlled manually with an air-operated control valve. The pressure switches are connected to an annunciator that warns when the oil pressure deviates from a preset range; a solenoid valve in the line enables the oil flow to be stopped rapidly.

The primary oxygen flow is measured by a calibrated rotameter and is controlled manually by a needle valve. The pressure switch in the oxygen line is connected to the annunciator panel to indicate a low-pressure oxygen supply; a solenoid valve enables the oxygen flow to be stopped rapidly.

The system was piped to provide for either air or oxygen atomization. The atomizing flow rate was measured by a calibrated rotamete Electric resistance heaters were installed in both the primary oxygen and the atomizing lines so that these streams could be heated during cold-weather operation.

Figure 6 shows a schematic diagram of the electrical wiring for one burner system. The pressure switches are connected to an annunciator that rings an alarm and flashes a light when any of the supply pressures deviate from a preset range. The solenoid valve switches are arranged so that the atomizing gas flow has to be started before the oil and oxygen to provide a safe start-up.

To become familiar with the operating characteristics of the burner, tests were made using only air and No. 6 fuel oil. A typical chemical analysis of the No. 6 fuel oil is shown in Table I. Although the burner performed as expected under complete-combustion conditions, burner operation became unstable as the air rate was decreased. Apparently, the heat released per unit volume of fuel became so low that the flame could not propagate itself effectively. The next step was to use oxygen for primary combustion gas and air for atomization.

During these initial tests using oxygen, the burner was being fired at 40 to 50 pounds of oil per hour using zero to 10 percent excess oxygen, and with an atomizing pressure of 40 to 60 psig. The pressure drop across the windbox of the burner (a measure of the energy

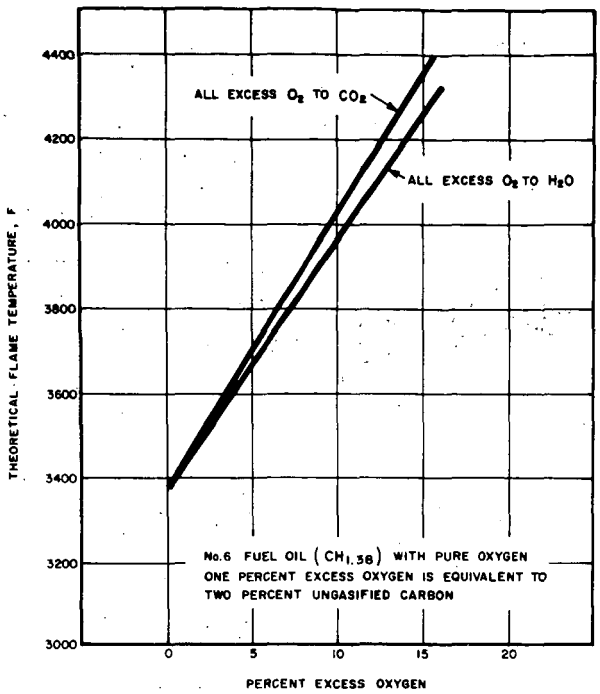

FIGURE 1 THEORETICAL FLAME TEMPERATURES FOR PARTIAL COMBUSTION OF BUNKER C FUEL OIL VERSUS EXCESS OXYGEN

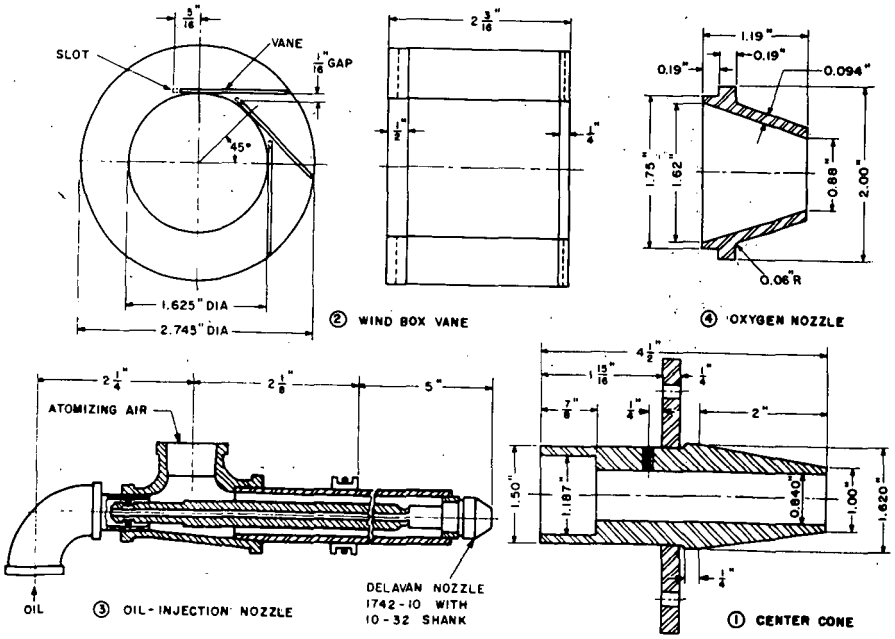

FIGURE 2 DETAILS OF BURNER PARTS

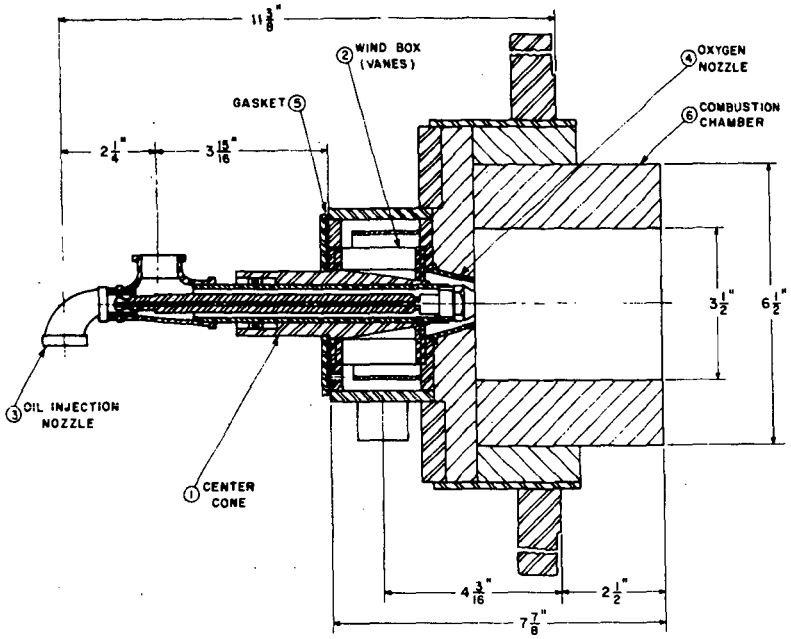

FIGURE 3 SECTION VIEW OF ASSEMBLED BURNER

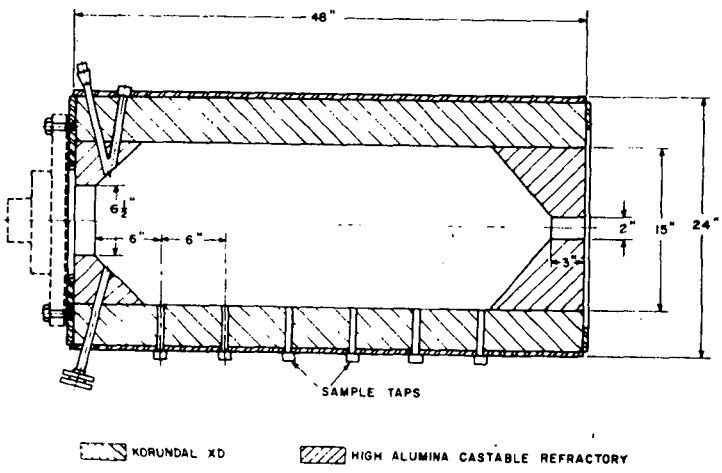

FIGURE 4 ATMOSPHERIC TEST CHAMBER

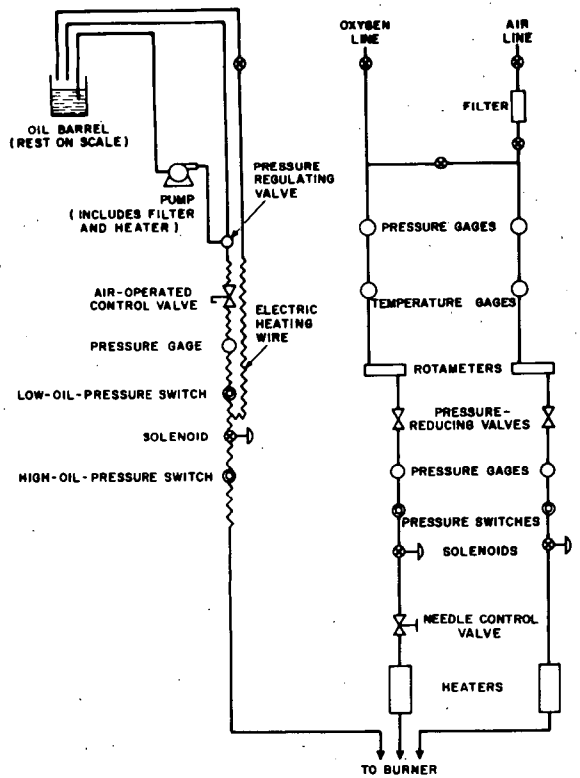

FIGURE 5 PIPING DIAGRAM FOR PARTIAL-COMBUSTION BURNER

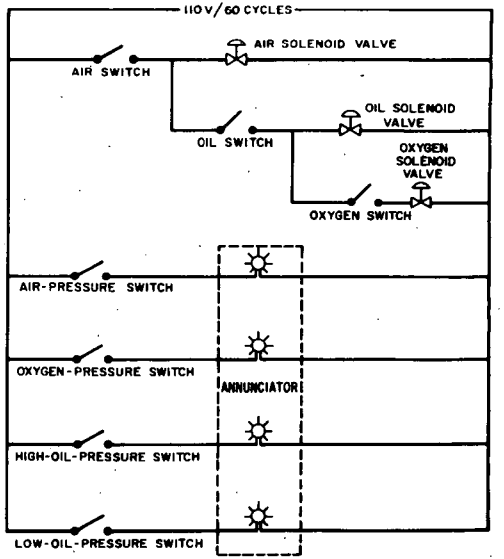

FIGURE 6 SCHEMATIC ELECTRICAL DIAGRAM FOR PARTIAL-COMBUSTION BURNER SYSTEM

released to the gas stream for mixing the reactants) was approximately two inches of water. In addition to poor conversions (the fraction of carbon in the oil that is gasified) during these studies, hard carbon would rapidly build up in the combustion chamber. This would direct the flame back onto the burner tip and force a shutdown. The hard carbon build-up was attributed to a combination of coarse atomization and lack of turbulence in the chamber, and probably occurred when oil droplets impinged on the hot refractory surface. It was obvious that finer atomization and increased turbulence in the chamber were necessary to prevent formation of hard carbon. Finer atomization was obtained by increasing the atomizing pressure. Increased turbulence in the combustion chamber was obtained by increasing the pressure drop across the windbox. This was done by decreasing the gap between the vanes in the windbox (part 2, Figure 2) from 1/16 inch to 1/64 inch, and decreasing the diameter of the oxygen nozzle (part 4, Figure 2) from 1 inch to 0.88 inch. These changes eliminated the hard-carbon build-up, but did not appreciably improve conversion. It was later determined that erosion of the nozzle tip had been the major cause of coarse atomization at 40 psig atomizing pressure, and that satisfactory operation at this atomizing pressure was possible with a new nozzle. When these changes were made it was possible to operate the burner continuously for extended periods (at least 8 hours) and a test program was begun to determine the operating conditions for most efficient fuel conversion. The independent variables chosen were oil rate, percent excess oxygen, and atomizing pressure. The range of conditions studied are listed in Table II.

Testing began when the walls of the atmospheric test chamber became incandescent. The independent variables chosen for the test were established and 30 minutes was allowed for attainment of steady-state conditions. Two gas samples, one 3 feet and one 1.5 feet from the burner nozzle, were then taken from the inside wall of the test chamber using an uncooled 1/4-inch-diameter stainless-steel tube. These samples were analyzed by gas chromatography for CO, CO_2, H_2, and N_2. Several samples were analyzed with a mass spectrometer to determine the quantities of other hydrocarbons (such as CH_4, C_2H_2, and C_2H_6) being formed. The mass-spectrometer results indicated that less than 1.5 percent of the total product gas was made up of constituents other than CO, CO_2, H_2, and N_2; the chromatograph results were therefore used to calculate material balances. Elemental balances for hydrogen, carbon, and oxygen were used to calculate the quantities of soot and water vapor, and the total moles of dry gas formed. A check on the consistency of the data was possible by a nitrogen balance.

Analysis of the data from this program showed that the burner was not very efficient (cf. results below). Because it was believed that the original nozzle was the major source of trouble, studies were also made using a special spray nozzle designed for operation over a wider range of fuel rates. Figure 7 is a detailed drawing of this nozzle.

Results of Burner Tests

Most commercial burner systems are operated under complete combustion conditions and efficiencies are usually expressed as thermal output per unit of fuel consumed. In the case of partial-combustion systems, it is more meaningful to consider the degree of gasification of the fuel. In the present application this type of burner has a dual purpose — to produce reducing gas and to produce sufficient heat to melt the solid products in a smelting operation. Thus, the formation of a small amount of CO_2 and H_2O is not necessarily detrimental to the performance of the process. However, it is possible that any ungasified carbon leaving the combustion zone will remain as such in its passage through the reactor and thus represent an unrecoverable loss of energy. In the analysis of the present data, therefore, the percent excess oxygen was considered as the independent variable, the percent ungasified carbon as the dependent variable, and the fuel rate, atomizing pressure, and sampling location as the parameters.

Figure 8 shows the data obtained inside the test chamber 3.0 feet and 1.5 feet from the original nozzle tip while operating at an oil rate of 45 to 50 pounds per hour; atomizing pressure is the parameter. It is clear that atomizing pressure has little effect on fuel conversion, probably because atomizing pressure has little effect on the mixing of the oil and oxygen. This would not be true at very low atomizing pressures (up to about 20 psig) where atomization is coarse and the rate of evaporation becomes a limiting step in the burning process. It is concluded that for all the atomizing pressures studied, the fineness of atomization was sufficient to maintain an evaporation rate greater than the reactant mixing rate, thereby making burner performance independent of atomizing pressure. This result held at the higher oil rates and also for the special spray nozzle.

Figure 9 represents the data when considering the fuel rate as a parameter. It is clear that fuel rate has no significant effect on conversion. This result is probably due to the fact that the decreased residence time for the higher fuel rates is compensated for by increased turbulence and concomitant improvement in mixing.

Figure 10 is a plot of percent ungasified carbon versus percent excess oxygen for comparable data using the original nozzle and the special spray nozzle. Better conversions were obtained with the special spray nozzle.

In all cases, better conversions were obtained 3 feet from the nozzle tip than 1.5 feet from the tip. This distance would be expected to directly affect the conversion since the extent of mixing is a function of that distance (in terms of increased residence time). In addition, the burning times of the solid residue and soot are probably comparable to the residence time of the gas in the test chamber. Thus, even with perfect mixing, a difference in conversion would exist between the two sampling locations.

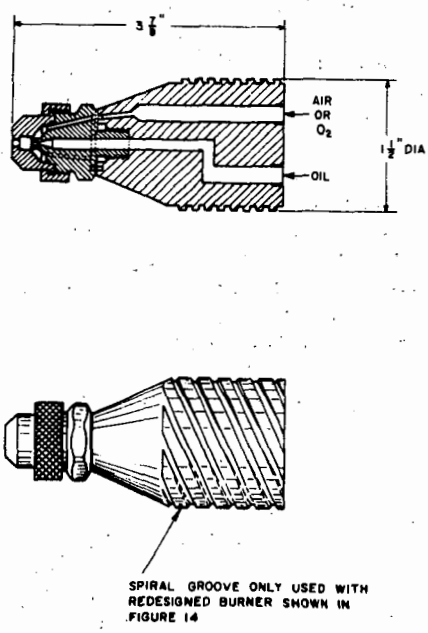

FIGURE 7 SPECIAL SPRAY OIL INJECTION NOZZLE

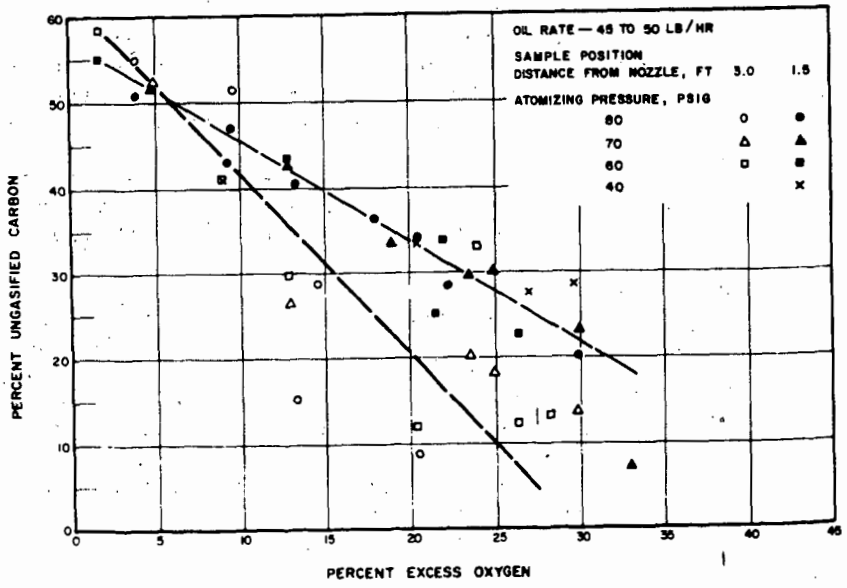

FIGURE 8 EFFECT OF ATOMIZING PRESSURE AND SAMPLING POSITION—ORIGINAL NOZZLE

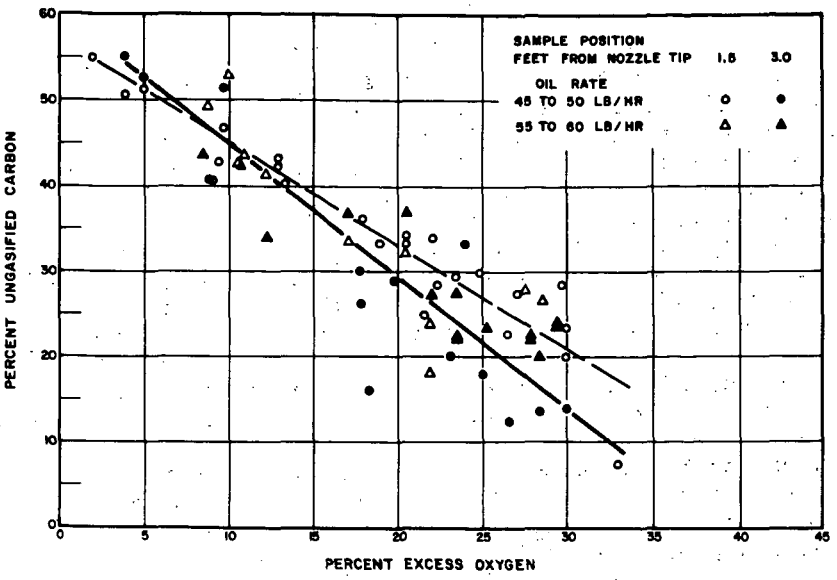

FIGURE 9 EFFECT OF FUEL RATE AND SAMPLING POSITION— ORIGINAL NOZZLE

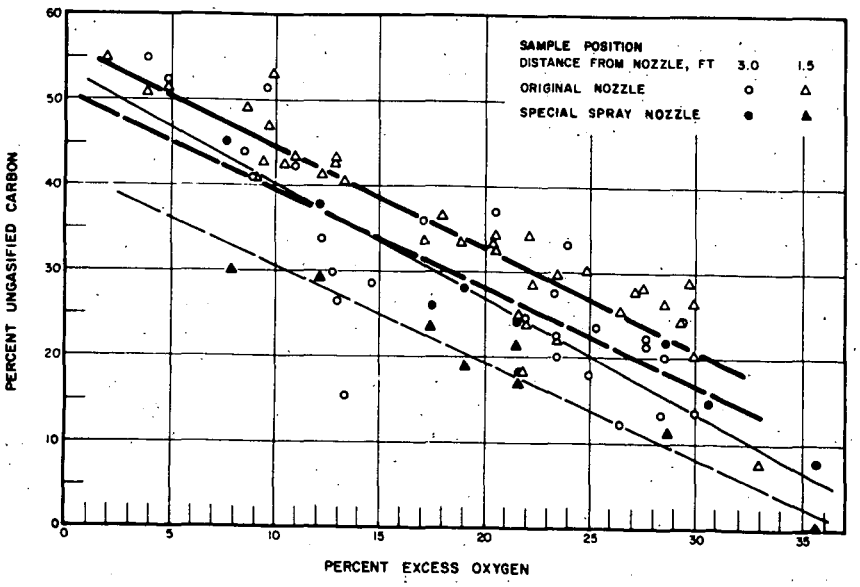

FIGURE 10 EFFECT OF SAMPLING POSITION AND NOZZLE DESIGN

Under all conditions, with less than 15 percent excess oxygen, the ungasified carbon was greater than 20 percent. With ideal mixing of the reactants, any ungasified carbon would represent solid carbon from nonvolatile matter in the oil and not from cracking of the volatiles. However, the oil contained greater than 90 percent volatile matter. Thus, at least half of the ungasified carbon formed came from cracking of volatiles. This is so because, with perfect mixing, the volatiles would probably burn as rapidly as they evaporate,[5] and the quantity of ungasified carbon would be 10 percent or less, depending on the sampling position and burning time of the residue.

The results of other work done on evaporation rates and combustion rates of fuel droplets[3] indicate that 0.3 to 0.6 seconds (the average residence time available for a drop to react in our apparatus) is far in excess of the time needed to evaporate and burn the volatile matter. It is therefore believed that the present system could, with perfect mixing of the reactants, gasify all carbon contained in the volatile matter and produce a product gas containing less than 10 percent ungasified carbon. Because gasification of solid residue is about 10 times slower than gasification of volatiles, conversions better than 90 percent would require longer residence time than can be obtained in the test chamber. In any event, the technical feasibility of the proposed smelting process should not be restricted by the low conversions obtained in the test chamber. This conclusion is based on the knowledge that, even when operating with 20 percent excess oxygen, the gas produced will be reducing to FeO. Table III shows the results of a representative run and a comparison of the actual CO_2/CO and H_2O/H_2 ratios with the equilibrium ratios for 2000 F. Although the H_2O/H_2 ratio is only moderately reducing, the CO_2/CO ratio is substantially reducing to FeO. In addition, it must be remembered that the operation of the proposed process will provide enough solid carbon in the burden to reduce these complete combustion products and for solution in the hot metal produced.

Pilot-Plant Design

Figure 11 is a picture of the pilot plant comprising of a shaft reactor, a double-hopper arrangement for feeding solids, an off-gas system, and a control room that houses most of the equipment for operating the burners. Figure 12 shows a cross-sectional diagram of the reactor, which is constructed in four sections: the hearth, the lower stack (containing two diametrically opposed burner mounting assemblies), the upper stack, and the top head. The reactor shaft is a 10-foot straight section, 1 foot in diameter, that flares to 2 feet where it is attached to the hearth. The hearth is 2 feet in diameter and 2 feet high. The reactor is lined with 18 inches of refractory material; the inner face of high-alumina brick is backed by a layer of fire-clay brick and a layer of low-conductivity castable refractory. The refractory is separated from the steel shell by a one-inch layer of asbestos block insulation.

Eight flanged ports for measuring stack temperatures and pressures, and for obtaining gas samples are located at four levels of the stack.

Table I

Chemical Analysis of No. 6 Fuel Oil

	Weight Percent
Carbon	87.24
Hydrogen	11.19
Oxygen	0.69
Nitrogen	0.27
Sulfur	0.59
Ash	0.02
Volatile Matter	94.56
Fixed Carbon	5.42

Table II

Range of Variables Studied in the Test Chamber

Oil Rate, lb/hr	Atomizing Pressure, psig	Excess Oxygen, %
48	80, 70, 60, 40	0 to 30
58	80, 70, 60	0 to 30

Table III

Results of Representative Burner Operation with No. 6 Fuel Oil

Test Number 181

Oil Rate	56.4 lb/hr
Atomizing Air Rate	3.39 scfm*
Primary Oxygen Rate	15.05 scfm
Excess Oxygen	21.6%
Ungasified Carbon	17.0%

Product Gas Analysis, Mole Percent

CO_2	5.5
CO	43.1
H_2	27.7
H_2O	17.2
N_2	6.5

$\frac{CO_2}{CO} = 0.128$ $\qquad$ $\frac{H_2O}{H_2} = 0.621$

$\frac{CO_2}{CO}_{eq} = 0.390$ $\qquad$ $\frac{H_2O}{H_2}_{eq} = 0.675$

Equilibrium ratios are for 2000 F

* 70 F and 1 atm

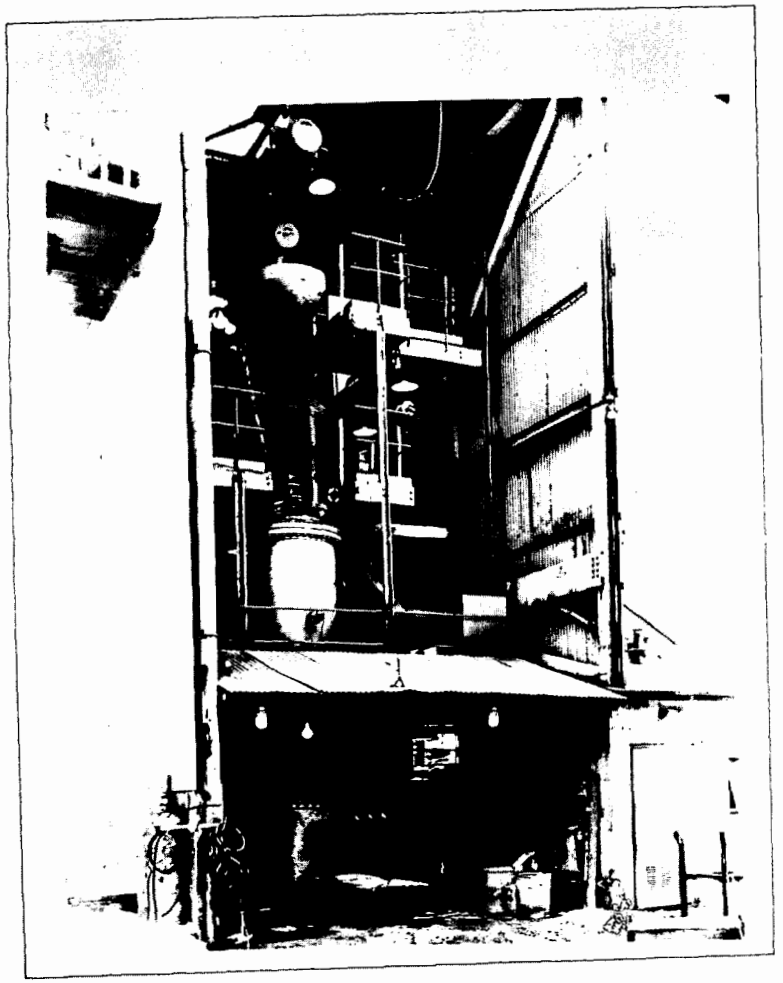

Figure 11. Picture of Pilot Plant

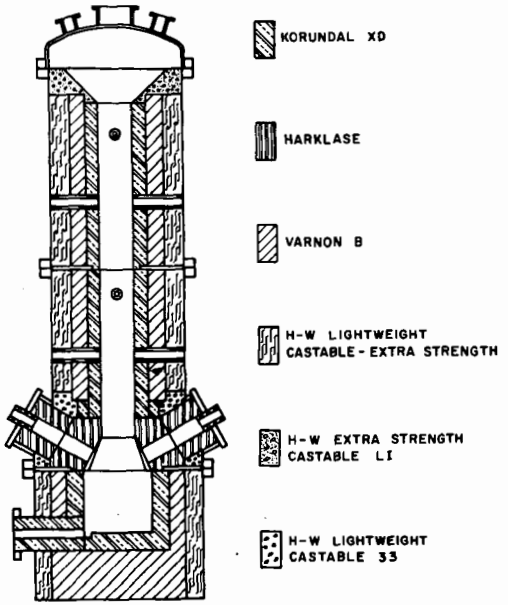

FIGURE 12 CROSS-SECTION OF FUEL-OIL OXYGEN SMELTING REACTOR

Partial-Combustion Studies in Pilot Plant

In the atmospheric test chamber the combustion efficiency (expressed as the percent of carbon gasified) was low; at least 15 percent excess oxygen (over the theoretical oxygen for combustion to CO and H_2) was needed for 80 percent gasification. These low conversions were caused by the low residence times and high heat losses in the test chamber. In addition, it was learned that the oil rate and the atomizing pressure had very little effect on the combustion efficiency. The percent excess oxygen and the residence time were the only variables that significantly affected combustion efficiency; gasification increased with increased excess oxygen and further distance from the burner.

A test program was run in the pilot plant to verify and extend the results obtained in the atmospheric test chamber. The ranges of the independent operating variables are listed in Table IV. Each burner test consisted of two hours of operation at the test conditions. A set of gas samples (bottom, top, and off-gas) was taken after one hour and after two hours of operation. Material balances were then calculated from the operating data and chemical analysis of the samples.

The results are plotted in Figure 13 as percent ungasified carbon versus percent excess oxygen for the special spray nozzle and for the original nozzle. The results obtained in the atmospheric test chamber are also shown for comparison. Conversions in the reactor were much better than in the test chamber because of the longer residence time and higher temperatures. Conversions for the special spray nozzle were significantly better than for the original nozzle. As in the atmospheric-test-chamber operation, there was no significant effect of the atomizing pressure or the oil rate on the burner performance.

There is considerable scatter in the data in Figure 13. This scatter is attributed primarily to poor gas mixing and distribution and to the fact that the material balances are very sensitive to small differences in nitrogen concentration. It is therefore instructive to study the results of a 24-hour test with constant-burner operating conditions. Gas samples were taken at the bottom and top of the reactor, and from the off-gas line every hour during this run. The other operating variables were recorded periodically so that an average material balance could be calculated for the day of operation. The material flows were held constant during the whole operation; there was less than 5 percent variation in any of the flows. The average operating data and results are presented in Table V. There was more ungasified carbon at the bottom of the reactor than at the top or in the off-gas. This result was expected because the studies made in the atmospheric test chamber showed that gasification increased with longer residence times. The increase in ungasified carbon between the top and the off-gas sections was unexpected and may be due to carbon deposition in this part of the system. Most of the short-duration tests in the reactor showed this same trend; there was a slightly higher amount of ungasified

Table IV

Operating Ranges for Burner Test Program

Excess Oxygen, %	- 5 to 25
Oil Rate, lb/hr	40 to 90
Atomizing Pressure, psig	40 to 70
Sampling Position	Bottom of Reactor
	Top of Reactor
	Off-Gas System

Table V

Summary of Average Operating Conditions and Results of 24-Hour Burner Test (2 Burners)

Oil Rate	73.4 lb/hr/burner
Atomizing Air Rate	6.57 scfm/burner
Primary Oxygen Rate	18.23 scfm/burner
Atomizing Pressure	70 psig
Percent Excess Oxygen	17.7

Dry-Gas Analyses, Vol. %	Bottom	Top	Off-Gas
CO	52.6	51.9	52.3
CO_2	4.1	3.2	3.2
H_2	34.6	36.4	35.8
N_2	8.7	8.5	8.7

Wet-Gas Analyses, Vol. %	Bottom	Top	Off-Gas
CO	46.4	49.6	48.9
CO_2	3.5	3.1	3.0
H_2	30.5	34.8	33.5
H_2O	11.9	4.4	6.3
N_2	7.7	8.1	8.2
Percent Ungasified C	10.0	-3.1	0.1

Nitrogen-Balance Error $\sim$ 0.7%
(Independent Data Check)

carbon in the off-gas line than at the top of the reactor and conversions at both of these locations were much higher than at the bottom of the reactor.

These results of the burner tests run with an unfilled reactor are summarized as follows:

1. Burner rates were varied from 40 to 90 pounds of oil per hour with no significant difference in burner performance.

2. Atomizing pressures were varied from 40 to 70 psig with no significant difference in burner performance.

3. Stable burner operation was obtained from minus 10 to plus 25 percent excess oxygen.

4. The burners could be operated continuously for at least 5 days with no noticeable nozzle erosion.

5. Combustion chambers cast from high-purity magnesium oxide and burned at about 2800 F performed very well.

Burner Redesign

Several problems associated with burner design were brought into focus during the reactor-test program. First, in the original design the combustion chamber was located very close to the outside mounting flange. Heat losses were therefore unnecessarily high and the mounting flange was susceptible to high-temperature damage. In addition, removal of the burner for inspection invariably broke the combustion chamber, and this meant a complete rebuilding of the burner. And finally, the inspection and replacement of burner nozzles that plugged during operation was time consuming.

Figure 14 shows a drawing of the revised burner design. This design eliminates all the problems discussed above without sacrificing any features of the original design that are necessary for efficient combustion. The combustion chamber was relocated closer to the stack, thereby minimizing heat losses and protecting the mounting. The unitized system could be quickly removed and replaced if any trouble occurred; also, the system retained the vortex action of the primary oxygen input.

Operation of Pilot Plant as a Steel Melter

After the operation of redesigned partial-combustion burners was demonstrated to be satisfactory with a coke-filled stack, it was planned to study the operation of the system as a steel melter. Steel punchings 1 inch in diameter and 3/8-inch high and small coke were used as the burden. The pilot plant was operated successfully as a melter for four consecutive days (including one day for start-up). Table VI presents a summary of the operating conditions and results. The oil rate during

Table VI

Summary of Operating Conditions and Results for Melting Operation

	Period 1	Period 2
Duration, hours	42	24
Oil Rate, lb/hr	100	100
Atomizing Air Flow, scfh	720	720
Atomizing Pressure, psig	~70	~70
Primary Oxygen Flow, scfh	1530	1530 (100% O_2)
Excess Oxygen, %	~20	~20
Theoretical Flame Temperature, F	4275	4275
Burden Ratio, lb coke/lb steel	0.25	0.11
Approximate Casting Rate, lb/hr	85	160

Oil Analysis, wt %	
C	87.03
H	11.09
N	0.29
O	0.95
S	0.59

Metal Analysis, wt %		
	Charge	Product
Fe	98.9	~98
Si	0.13	<0.01 to 0.29
S	0.031	0.11 to 0.18
C	0.37	0.2 to 2.6

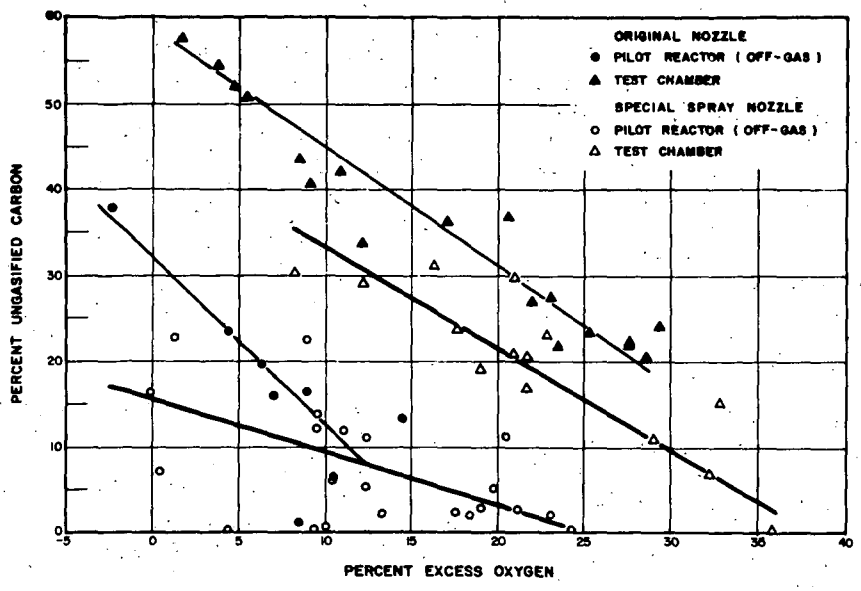

FIGURE 13 CONVERSION VERSUS EXCESS OXYGEN

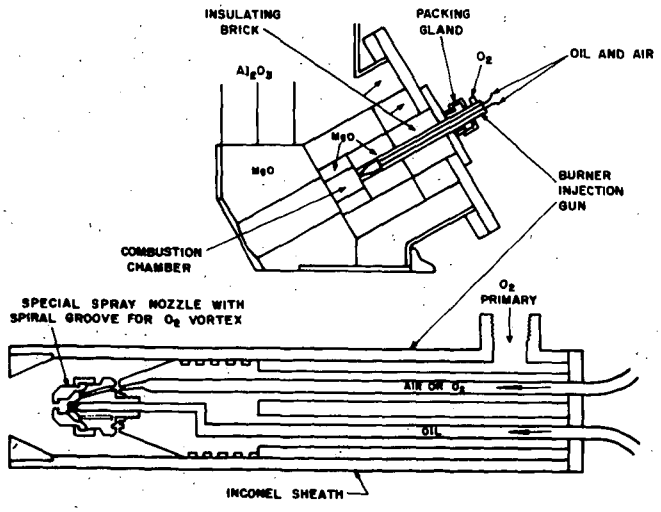

FIGURE 14 SCHEMATIC DIAGRAM OF NEW BURNER DESIGN

this operation was 100 lb/hr (for two burners); the burners were operated with about 20 percent excess oxygen, and the atomizing air pressure was 70 psig. The burden movement was smooth, and hot metal was successfully removed from the hearth during this operation. During the first day and a half of melting operation, the coke-to-steel weight ratio was 0.25 and the melting rate was 85 lb/hr. During the rest of this period, the coke-to-steel ratio was decreased to 0.11 and the melting rate was 160 lb/hr. Inspection of the system after the shutdown showed that the reactor and the burner guns were in excellent condition.

Operation of Pilot Plant as a Smelter

The pilot plant was operated as a smelter with a burden of 90 percent self-fluxing sinter and 10 percent coke. Table VII presents a summary of the steady-state operating conditions and results. About 12 hours after the first charge, small amounts of molten metal were tapped. The rate of burden movement gradually increased for the next 7 hours until it reached a steady state. For the next 13 hours operation was very good. The charging rate averaged 340 lb/hr and was very steady. Casts were made every two hours and little difficulty was encountered in getting the material to flow. Operation of the burner was very smooth. The operation ended when the burden hung at the base of the feed hopper and then slipped 1-1/2 hours later, thereby charging 500 pounds of cold material into the stack. This plugged the stack and caused a complete shutdown. Considerable damage was done to the refractory in the hearth and lower stack.

As shown in Table VII, the total carbon rate was 1300 lb/THM, of which the coke supplied about 300 lb/THM, and the fuel oil 1010 lb/THM. This low total fuel and coke ratio is very encouraging because of the small size of the pilot reactor, which inherently has relatively large heat losses. Also encouraging was the fact that burden movement was excellent in spite of the low coke ratio, and there were no indications that an even lower coke ratio would not work well.

Many serious problems were encountered during the operation of the pilot plant, primarily with the construction and performance of the refractories around the burners. There were many failures; however, it is believed that these failures can be attributed to the small size of the plant. Because the plant has a relatively high ratio of surface area to volume, heat losses were high and the burners must be operated at higher temperature (higher excess oxygen) to compensate. In a larger plant the operating conditions would not be as severe. In any event, the results indicate, at least from the standpoint of burden movement and permeability, that very high "fuel-injection" levels — approaching "cokeless" operation — can be achieved in shaft processes for smelting iron ore.

Table VII

Summary of Operating Conditions and Results
For Smelting of Self-Fluxing Sinter

A. Raw Material Analyses, Weight Percent

Coke		Sinter		No. 6 Fuel Oil	
C	88.26	Fe_T	60.52	C	87.36
H	1.82	O	24.50	H	10.92
N	0.96	SiO_2	5.72	O	0.87
S	0.75	Al_2O_3	1.02	Ash	0.012
O	2.55	CaO	6.93	S	0.55
Ash	5.66	MgO	0.89		
Moisture	8.53	TiO_2	0.15		
		C	0.15		
		S	0.009		
		M_m	0.093		
		P	0.054		
		FeO	11.91		
		Fe_2O_3	73.29		

Combustion Oxygen 99.5 percent O_2

B. Input Data

No. 6 Fuel Oil, lb/hr	119.1	
Coke, lb/hr	37.8	
Sinter, lb/hr	340.0	
Atomizing Air, moles/hr	1.73	(11.16 scfm)
Primary Oxygen, moles/hr	4.78	(30.82 scfm)

C. Output Data

Average Off-Gas Analysis (approximate volume %, based on 3 samples), Dry Basis

CO	49.0
CO_2	12.7
H_2	28.25
N_2	9.9

Material Balance - Based on N_2

Dry Volume	14.0 moles/hr
H_2O	2.96 moles/hr
Total soot plus dissolved carbon	2.6 moles/hr

Table VII

(continued)

Summary of Operating Conditions and Results
For Smelting of Self-Fluxing Sinter

Independent Oxygen Balance

Input	=	Output
7.83 moles/hr	=	6.69 moles/hr

D. General Data*

Solid Carbon Consumption, lb/hr	30.5
Solid Carbon Ratio, lb/THM	~298
Total Carbon Consumption, lb/hr	134.5
Total Carbon Ratio, lb/THM	~1312
Metal Rate, lb/hr	~205

*Metal rate based on input

References

1. Masdin, E. G., and Thring, M. W., "Combustion of Single Droplets of Liquid Fuel," Journal of the Institute of Fuel, Vol. 35, No. 257, p 251, June 1902.

2. Thring, M. W., The Science of Flames and Furnaces, pp. 198, 199, 256, John Wiley and Sons, Inc., Second Edition, 1906.

3. Masdin, E. G., and Thring, M.W., ibid, pp. 254, 255.

"THE REACTION OF COKE WITH CARBON DIOXIDE"

H. C. Hottel, G. C. Williams and P.C. Wu

Chemical Engineering Department
Massachusetts Institute of Technology
Cambridge, Massachusetts 02139

Earlier studies of the kinetics of the CO_2-C reaction have generally been deficient for one or both of two reasons: either the data were based on imprecise methods of determining the extent of reaction (e.g., product gas analysis, reactant weight decrease, pressure variation) or the data did not yield information concerning local- or point-reaction rates, which are the kind of data required for formulating kinetic mechanisms. Most commonly the data were on reaction in a tube of finite length, packed with carbon.

The present studies were of mono-layers of carbon particles resting on a screen up through which the reactant gas mixtures were passed, the system being maintained isothermal. Details of the apparatus and experimental techniques are given by Wu (1). The reactant gases were CO_2, CO_2-N_2 mixtures, and CO_2-CO mixtures. Before each run the system was evacuated, following which reactant gas was passed through for 10 to 15 minutes. Because of the high reactivities of H_2O and O_2 relative to CO_2 the gas mixture was dried by passage through a bed of Drierite and then stripped of trace oxygen by contact with reduced copper turnings at 415°C. After the furnace had reached the desired temperature level the screen with the carbon particles was introduced by a magnetically operated slide mechanism the smooth operation of which prevented disturbance of the carbon bed. After a specified time the carbon bed was quickly removed, cooled and weighed. The decrease in weight of the carbon and the time of reaction were used to determine the specific reaction rate for each run.

The solid reactant used was from the same lot used by Gilliland et al (2) and by Graham (3) in fluidized beds. The effect of particle size from 80-100 mesh to 10 mm diameter was determined in the present studies. The coke contained 9.5 weight per cent ash and a small percentage of V.C.M. Reaction rates, R, mg c/g.c. min., are expressed on an ash-free basis and corrected for loss of V.C.M. as a function of reaction time, temperature and particle size on the basis of experiments made in pure N . The maximum weight loss correction for V.C.M. amounted to 1.5% of the initial weight of the particles.

The various reaction rate terms used are defined as follows:

(1) The instantaneous specific reaction rate R_i is defined as the rate of decrease in weight of carbon based on unit weight W of carbon at the fractional residual carbon W_o-W/W_o = F:

$$R_i = \frac{-dW}{W\,d\theta} = \frac{-d\ln W}{d\theta} = \frac{-d\ln(1-F)}{d\theta} \qquad (1)$$

(2) The initial specific reaction rate R_o is defined as the rate of decrease in weight of carbon based on unit weight of carbon at F=0:

$$R_o \equiv -\left(\frac{dW}{W\,d\theta}\right)_{F=O} \equiv -\left(\frac{d\ \ln\ (1-F)}{d\theta}\right)_{F=O} \equiv \left(\frac{dF}{d\theta}\right)_{F=O} \qquad (2)$$

(3) The average specific reaction rate R_{av} is defined as the time mean of the instantaneous specific reaction rate R_i from F=O to F=F;

$$R_{av} \equiv \frac{\int_o^\theta R_i d\theta}{\theta} \equiv \frac{\int_o^\theta -\frac{dW}{W\,d\theta}\,d\theta}{\theta} \equiv \frac{\int_{W_o}^{W} -\frac{dW}{W}}{\theta} \equiv \frac{-\ln\ (1-F)}{\theta} \qquad (3)$$

The experimental results, all obtained at a total pressure of 780 mmHg, can be classified into the following two groups:

1. Experiments using New England coke particles of 50-60 mesh.

The gas flow rate, except in the velocity runs, was maintained constant.

(a) N_2 blank runs: Typical results are listed in Table 1, as fractional decrease in weight of the sample, F_{N_2}, calculated from the data on an ash-free basis at different temperatures.

(b) CO_2-N_2 runs: Five temperatures (1500, 1600, 1700, 1800 and 1900°F) were investigated. The time of reaction was adjusted for each run to give approximately 10% reaction. In Figure 1 the values of the average specific reaction rate R_{av} are plotted vs the partial pressure of CO_2 on semi-logarithmic coordinates. For each pair of curves the upper one shows R_{av} calculated on an ash-free basis, and the lower one shows that calculated on an ash-free basis, after being corrected for V.C.M. based on the N_2 blank runs.

(c) CO_2-CO runs: These data are shown in Figure 2.

(d) Velocity runs: The temperatures investigated were the same as in the CO_2-N_2 runs. Since the gas flows were in the laminar region a linear plot of R versus the reciprocal of the gas flow rate gave straight lines which could be extrapolated on a straight line through the data points to the origin, corresponding to the reaction rate in pure CO_2, uncontaminated by the CO produced.

TABLE 1

Evolution of VCM as a function of time and temp. in N_2 50-60 mesh particles.

TEMP.°F	1500		1600		1700		1800				1900
$F_{N_2} \times 10^3$	8.8	7.9	10.3	8.1	15	11.6	19	14.5	11	9	6.7
θ, min	610	463	240	100	120	60	90	60	30	15	10

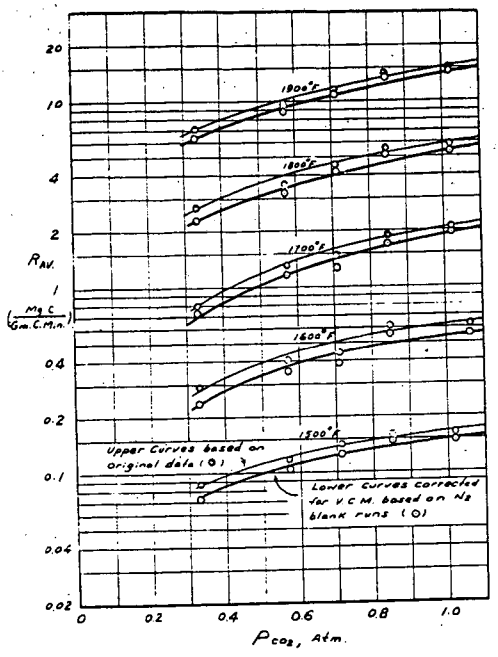

Figure 1. Effect of Partial Pressure of CO_2 and Temperature on Reaction Rate of 50-60 Mesh Coke Particles.
Total Pressure 1.006 atm, N_2 as Diluent.

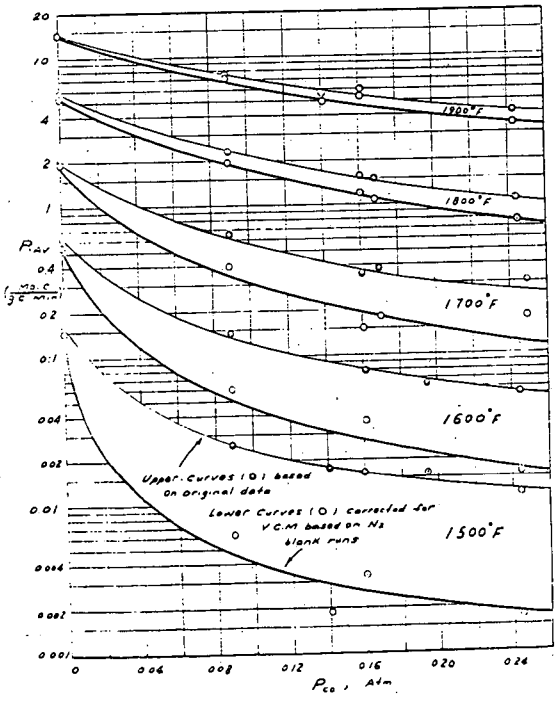

Figure 2. R_{av} vs. P_{CO} For CO_2-CO Runs
(New England Coke, 50-60 Mesh)

2. Experiments using New England coke particles of different sizes, reacting with pure carbon dioxide at 1800°F.

(a) N_2 blank runs: The fractional gasification in N_2 for the 8-12 mesh particles at any given time was about 60 per cent of that for the 50-60 mesh data shown in Table 1 and that for the 80-100 mesh particles was about 50 per cent greater. The effect of further increase in particle size up to nearly 10 mm diameter was a very small, less than 10 per cent decrease in gasification below that for the 8-10 mesh particles.

(b) Time runs: Reaction runs were made with samples of particle sizes between 8-100 mesh. Six different particle sizes were used, namely, 8-12, 16-20, 30-40, 50-60, 70-80, and 80-100 mesh. Each sample weighed about 0.1 gram. The values of R_{av} calculated from the corrected data are plotted vs θ in Figure 3 together with lines of constant F.

DISCUSSION OF RESULTS

Effect of Particle Size

From slopes of the curves of R_{av} vs in Figure 3 values of R_i were calculated and extrapolation of these to F=0 gave R_o. Values of R_o and the maxima of R_i are shown as a function of initial particle diameter in Figure 4.

From Figure 3 it is clear that the reaction rate is influenced not only by the fractional decrease in weight of carbon, F, but also by the diameter of the coke particle, D.

For all sizes investigated, R_i initially increased, reached a maximum, and then declined with further reaction. There was a pronounced trend for the maximum to occur at larger F values when smaller particles were used.

The shift of $R_{i(max)}$ to larger values of F with decrease in particle size can be explained as being due to the presence in the coke of ash, which amounts to 9.5%. In the case of the large particles, only a relatively small fraction of the weight of the particle has to be reacted to form a substantial layer of ash on the surface. The ash coating then makes the carbon less accessible to the reacting gas, and the reaction rate falls off. However, in the case of the small particles, a large fraction of the weight of the particle must be burned away to produce the substantial ash layer that retards further reaction.

The effect of initial particle size on the specific reaction rate as shown in Figure 3 may be explained as follows: (1) In the larger size range, 2-10 mm, the reaction occurs in a thin porous coke layer dependent in thickness on the ratio of the rate of diffusion of CO_2 into the particle to the rate of reaction on the surfaces of the pores but independent of particle diameters, thus the rate is proportional to the superficial surface area of the particles - a slope of minus unity in Figure 3. (2) As the particle size is further reduced, 1.5 to 0.5 mm, the thickness of the

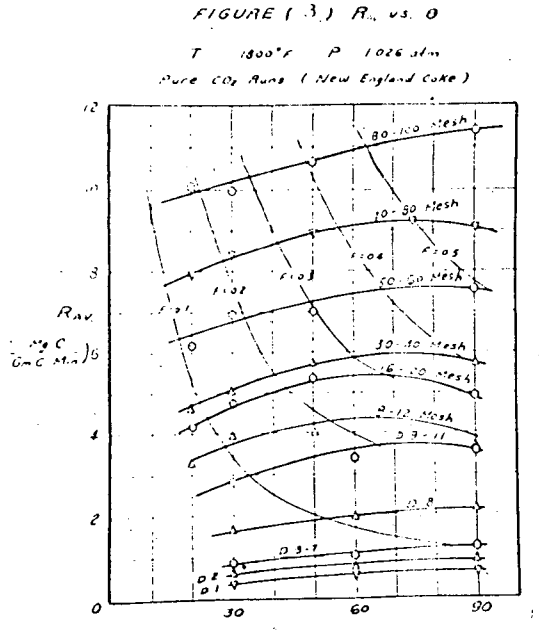

Figure 3. Effect of Time of Reaction and Particle Size on Average Reaction Rate in Pure CO_2 at 1800 F and 1.026 atm.

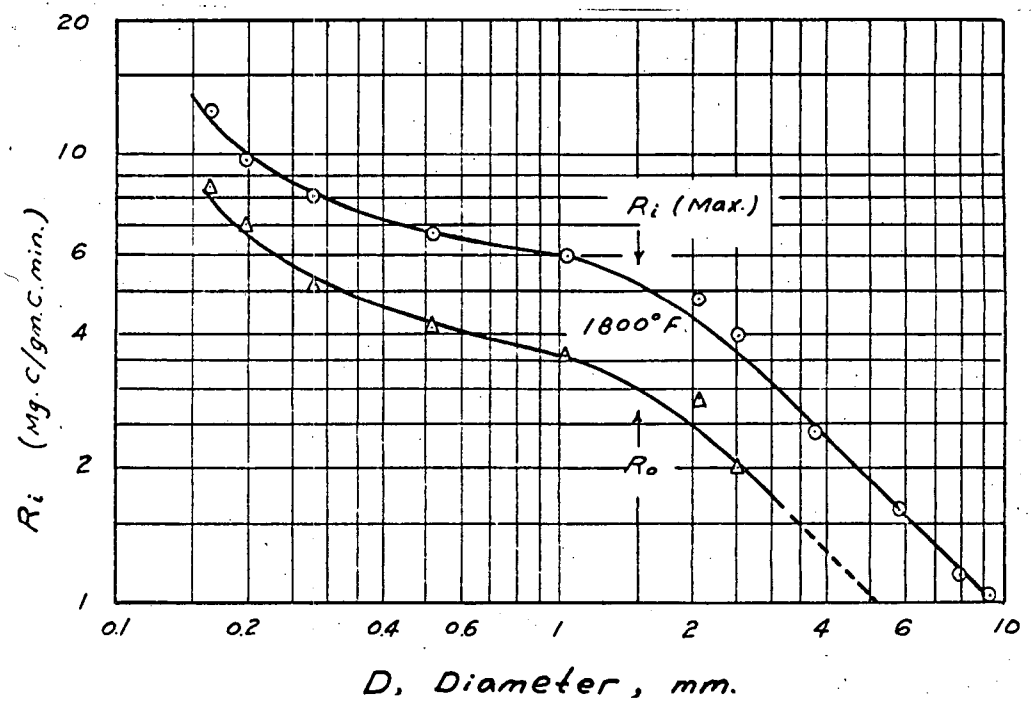

Figure 4. Effect of Size on Rate

diffusion-reaction zone becomes comparable with the particle radius and all of the particle volume becomes active, specific reaction rate becomes nearly independent of particle size. (3) With further decrease in particle size it is possible that the average depth of the pores in which reaction occurs is also reduced thus accounting for the increase in specific reaction rate as the particle size is reduced from 0.5 to 0.17 mm. It should also be noted that the initial apparent density of the coke particles (1.0 g/cc for massive particles) increased from 2.0 g/cc to 2.8 g/cc as the particle size was reduced in this size range, probably due to a loss of ash in the grinding and sieving process. This could also be advanced as an explanation for the increase in specific reaction rate as size decreases in this size range.

Effect of Fractional Reaction

In other experiments (1) with ash-free electrode carbon gasified in CO_2 it was found that, presumably because of an increase in surface area with progress of reaction, the instantaneous specific reaction rate was a linear function of the weight fraction gasified:

$$R_i = R_o\left(1 + \frac{m}{R_o} F\right), \quad \text{where } m/R_o \text{ was 14 for 50-60 mesh particles.}$$

In the present experiments the effect of the ash as shown in Figure 3 is apparently to accumulate to such an extent that the increase in surface area due to reaction is finally offset by the accumulation of ash.

The present data on coke can be correlated by the empirical expression

$$R_i = R_o\left(1 + \frac{m}{R_o} F\right) e^{-5.5DF^{1.85}}$$

in which the exponential represents the retarding effect of the ash and m is a function of initial particle diameter

$$m = \frac{10(2 + \log_{10} D)}{R_o}, \quad D \text{ in mm}$$

It is interesting to note that m for 50-60 mesh from this equation for coke is 13 vs the 14 reported for electrode carbon. The studies of Goring (4), Oshima and Fukuda (5) and of Duffy and Leinroth(17) show similar results on high-ash cokes.

Kinetics

1. Langmuir-Hinshelwood derivation

Hinshelwood et al (16) presented the following derivation as representative of the simplest application of the early ideas of Langmuir (6) on the effect of surface adsorption on heterogeneous reactions. Note that Langmuir himself did not present the following derivation, and in fact stated in 1915 (7) that he did not believe

carbon dioxide was adsorbed in the reaction of carbon with carbon dioxide. He gave instead the first step of the mechanism of Semechkova and Frank-Kamenetzky.

Hinshelwood et al made the assumption that both the reactant, CO_2, and the retarding product, CO, are adsorbed as such on the carbon surface, and that the rate of reaction is proportional to the fractions of the surface covered by the reactant. The mechanism can then be expressed by the following equations:

$$CO_2 \underset{k_2}{\overset{k_1}{\rightleftharpoons}} (CO_2) \qquad (4)$$

$$CO \underset{k_4}{\overset{k_3}{\rightleftharpoons}} (CO) \qquad (5)$$

$$C + (CO_2) \xrightarrow{k_5} 2CO \qquad (6)$$

in which equations, (...) represents gas in the adsorbed state.

The surface consists of equivalent and independent reaction sites, each of which can be occupied by one CO_2 or one CO molecule. When a steady state on the surface is attained, the rate of reaction per unit surface is then given by:

$$\text{Rate} = k_5 s_1 = \frac{\dfrac{k_5 k_1}{k_2 + k_5} P_{CO_2}}{1 + \dfrac{k_3}{k_4} P_{CO} + \dfrac{k_1}{k_2 + k_5} P_{CO_2}} \qquad (7)$$

2. Derivation of Semechkova and Frank-Kamenetzky (8)

The assumptions made are that carbon dioxide is not adsorbed as such, but reacts with the carbon to give an atom of oxygen which remains on the surface, and a molecule of carbon monoxide which passes into the gas phase. The adsorbed oxygen atom, taking up an atom of carbon from the surface forms gaseous carbon monoxide at a steady rate. Carbon monoxide present in the gas phase is always in equilibrium with carbon monoxide in the adsorbed state on the surface (this is the sole part of the reaction scheme which is identical with the previous derivation). There is a distinction between the adsorbed oxygen and the adsorbed carbon monoxide. The following equations express the mechanism:

$$C + CO_2 \xrightarrow{k_6} CO + CO^* \qquad (8)$$

$$CO^* \xrightarrow{k_7} CO \qquad (9)$$

$$CO \underset{k_4}{\overset{k_3}{\rightleftharpoons}} (CO) \qquad (10)$$

in which CO* represents an O atom adsorbed on carbon, and (CO) represents CO in the adsorbed state.

When a steady state on the surface is attained, the rate is found to be:

$$\text{Rate} = k_7 s_3 = \frac{k_6 P_{CO_2}}{1 + \frac{k_3}{k_4} P_{CO} + \frac{k_6}{k_7} P_{CO_2}} \qquad (11)$$

It is seen that also this expression is of the same form as equation (7).

3. Modified Semechkova and Frank-Kamenetzky Derivation (1)

In this derivation the assumption is also made that carbon dioxide is not adsorbed as such, but reacts with the carbon to form a gaseous carbon monoxide molecule, and an adsorbed oxygen atom, which is next transformed at a steady rate, not to gaseous CO, but to (CO), the adsorbed CO, the concentration of which on the surface is in equilibrium with the CO in the gas phase.

The following equations represent this mechanism:

$$C + CO_2 \xrightarrow{k_6} CO + CO^* \qquad (12)$$

$$CO^* \xrightarrow{k_8} (CO) \qquad (13)$$

$$CO \underset{k_4}{\overset{k_3}{\rightleftharpoons}} (CO) \qquad (14)$$

At steady surface state the following relations hold:

$$\text{Rate} = k_8 s_3 = \frac{k_6 P_{CO_2}}{1 + \frac{k_3}{k_4} P_{CO} + k_6 \left(\frac{1}{k_8} + \frac{1}{k_4}\right) P_{CO_2}} \qquad (15)$$

which equation is seen to be of the same form as (7) and (11) and of the general type

$$R = \frac{K_1 P_{CO_2}}{1 + K_2 P_{CO} + K_3 P_{CO_2}} \qquad (16)$$

The applicability of the Langmuir type equation can be tested, and the constants involved evaluated by application to the data obtained in both CO_2-N_2 and CO_2-CO runs shown in Figs. 1 and 2. It is evident that where the surface is completely characterized by F, as shown before, the instantaneous specific reaction rate at any F could be used for this evaluation. However, R_o was chosen as a reference value for testing the validity of the proposed Langmuir equation. The procedure used was as follows:

In the case of the CO_2-N_2 runs, the term $K_2 P_{CO}$ is 0, if the effect of the CO generated during the reaction can be neglected. The equation can hence be reduced and rearranged to:

$$\frac{P_{CO_2}}{R_o} = \frac{K_3}{K_1} P_{CO_2} + \frac{1}{K_1} \qquad (17)$$

If the proposed equation fits the data, then for a specific reaction temperature when P_{CO_2}/R_o is plotted vs P_{CO_2} on linear coordinates a straight line with slope K_3/K_1 and intercept $1/K_1$ should result, from which values of K_1 and K_3 can be evaluated. The data for 1900°F are shown in Figure 5; the intercept gives $K_1 = 28.6$ and the slope gives $K_2 = 0.56$.

When the equation is applied to the CO_2 - CO runs, rearrangement of the equation to a more convenient form is possible by substituting $P_{CO_2} + P_{CO} = \pi$, where π is the total pressure on the reaction system. The rearranged equation then becomes

$$\frac{P_{CO_2}}{R_o} = \frac{K_2 - K_3}{K_1} P_{CO} + \frac{1 + K_3 \pi}{K_1} \qquad (18)$$

For a specific reaction temperature when P_{CO_2}/R_o is plotted vs P_{CO} on linear coordinates, a straight line with slope K_2-K_3/K_1 and intercept $1+K_3\pi/K_1$ should be obtained. With the aid of the values for K_1 and K_3 calculated from the results of the CO_2-N_2 runs at the same temperature, K_2 can then be evaluated from the slope of this line. Figure 6 shows the 1900°F data, the slope is 0.6 from which $K_2 = 18$.

The data for the other temperatures were similarly treated and over the range of variables investigated, R_o for 50-60 mesh particles could be represented by a Langmuir type equation of the following form:

$$R_o = \frac{K_1 P_{CO_2}}{1 + K_2 P_{CO} + K_3 P_{CO_2}}$$

The values of K_1, K_2 and K_3 are listed in Table 2 and shown on logarithmic-reciprocal temperature coordinates in Fig. 6.

TABLE 2

Langmuir Equation Constants

(50-60 mesh)

	Reaction Temperature, °F				
Constants	1500	1600	1700	1800	1900
K_1 (mg.C/gm.C.min.atm)	0.23	0.9	3.18	10.2	28.5
K_2 (atm^{-1})	423	178	78	36	18.
K_3 (atm^{-1})	0.5	0.45	0.39	0.35	0.56

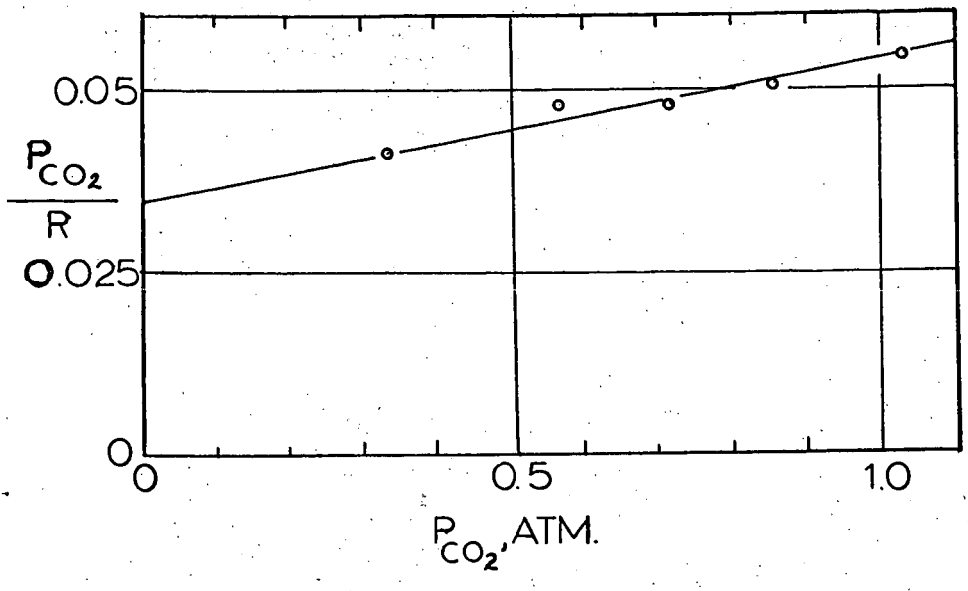

Figure 5. Test of Langmuir Isotherm
1900 F., 50-60 Mesh

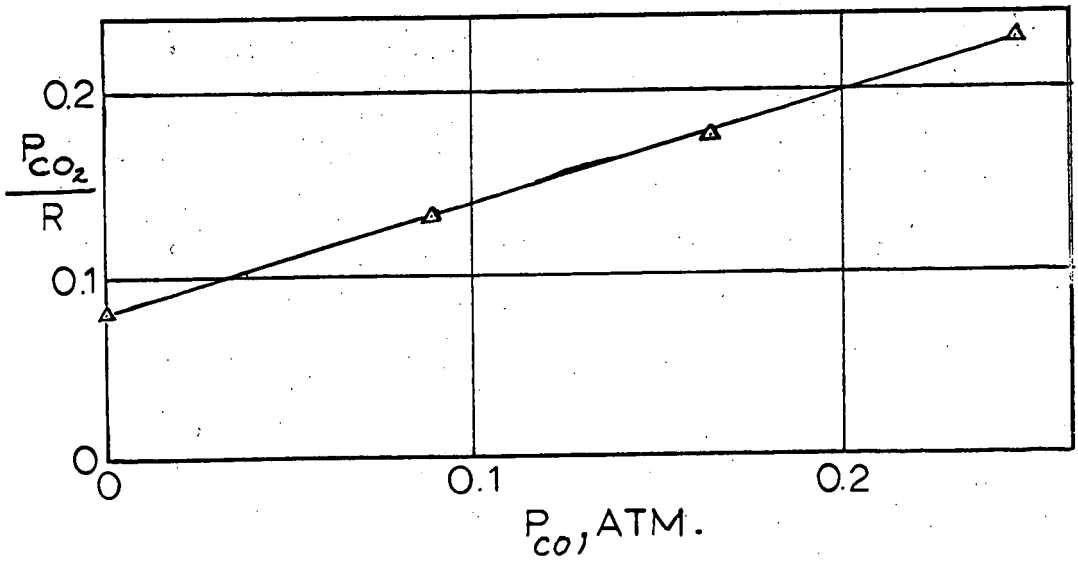

Figure 6. Test of Langmuir Isotherm
1900 F., 50-60 Mesh

From the straight line shown on Fig. 6 the values of K_o and E were calculated for each constant and are listed in Table 3 :

TABLE 3

Values of E and K_o in $K = K_o e^{-E/RT}$

(50-60 mesh)

E_1	111,000 (Btu/lb mole)	K_{10}	5.2×10^{11} (mg C/gm C min atm)
E_2	72,500 "	K_{20}	3.6×10^{-6} (atm^{-1})
E_3	11,000 "	K_{30}	3×10^{-2} (atm^{-1})

It is to be noted that, if the equation describes a rate affected by surface adsorption of CO and CO_2, i.e., if the Langmuir-Hinshelwood derivation is substantially correct, then the signs of the three E's are as expected. E_2 and E_3 are associated with adsorption phenomena which should become less important as the temperature rises, whereas E_1 (= E_r + E_3) is the primary measure of effect of temperature on reaction rate.

4. The Temkin adsorption isotherm

A major theoretical deficiency of the Langmuir adsorption isotherm is the implicit assumption of uniform heat of chemisorption and hence of surface activity. For most real surfaces the heat of adsorption changes with the degree of occupation of the surface (9), (10), (11) and (12). A linear decrease in heat of adsorption with fractional surface coverage leads to an isotherm for which the fractiona surface coverage is proportional to the logarithm of the pressure of the adsorbing gas. This isotherm has been named after Temkin (13) although the concept appears in the works of earlier Russians (14), (15)

If the heat of adsorption, q, falls linearly with the fraction of surface occupation, S,

$$q = q_o (1 - \beta S)$$

the isotherm is given by

$$S = \frac{RT}{q_o \beta} \ln A_o P \qquad (19)$$

where, β = a constant

q_o = a constant

$A_o = a_o e^{q_o/RT}$

a_o = constant

If it is assumed that chemisorption of CO_2 is fast compared with subsequent surface reactions and that the rate of surface reaction is directly proportional to the fraction of the surface covered then

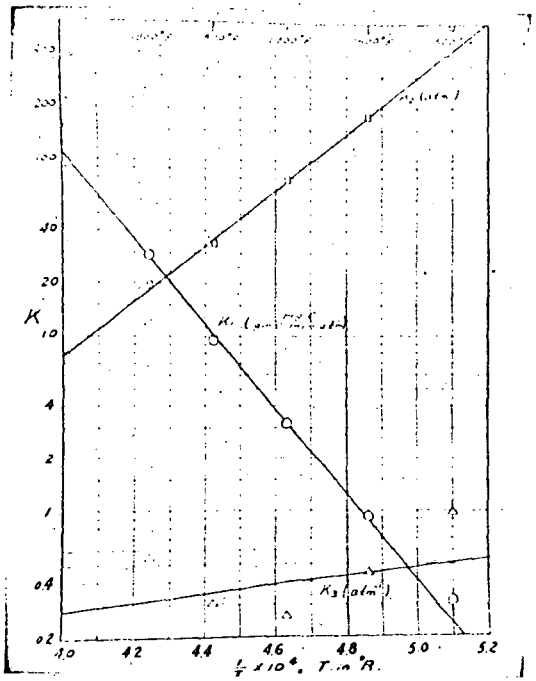

Figure 7. Arrhenius Plot of Reaction Rate Constants, 50-60 Mesh Coke.

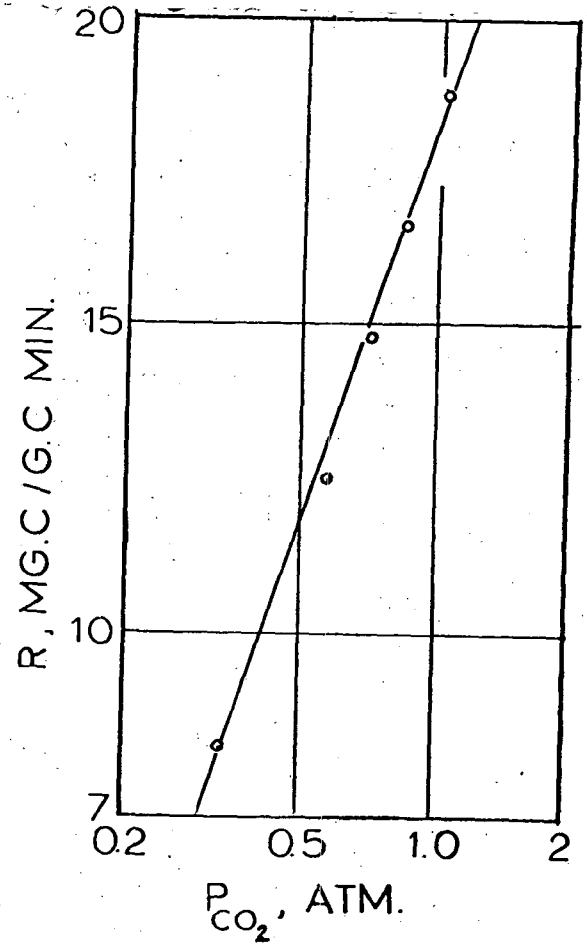

Figure 8. Test of Temkin Isotherm, 1900 F.

$$R_o = \frac{k\, e^{-E/RT}}{\beta\, q_o} RT \ln A_o + \frac{k\, e^{-E/RT}}{\beta\, q_o} RT \ln P_{CO_2} \qquad (20)$$

$$R_o = a(T) + b(T) \ln P_{CO_2} \qquad (21)$$

Thus a plot of reaction rate versus logarithm of the pressure should be linear. Fig. 7 shows the data for 50-60 mesh particles in pure CO_2 at 1900°F. The data for other temperatures are correlated equally well.

From Eqs. 19, 20 and 21

$$\frac{a}{b} = \ln a_o + \frac{q_o}{RT} \qquad (22)$$

Thus a plot of a/b versus 1/T should give a straight line with slope q_o/R. The present data give a value of heat of adsorption of CO_2 of 2400 Btu/lb mole and an intercept $\ln a_o = 1.4$ at $1/T = 0$.

Since q_o probably does not vary greatly with temperature b/T should be exponential in 1/T. This was found to be so, giving a value $b/T = 81 \times e^{-45,600/RT}$.

No attempt has been made to treat the CO_2-CO mixture data using the logarithmic adsorption isotherm.

ACKNOWLEDGEMENT

This work was supported by funds from Bituminous Coal Research, Inc.

LITERATURE CITATIONS

1. Wu, P. C. "The Kinetics of the Reaction of Carbon with Carbon Dioxide" Sc. D. Thesis, Chem. Eng., MIT (1949).

2. Gilliland, E. R., Lewis, W. K., McBride, G. T., Ind. Eng. Chem., 41, 1213 (1949).

3. Graham, H. S., "Gasification of Carbon by Steam and Carbon Dioxide in a Fluidized Powder Bed", Sc.D. Thesis, Chem. Eng., MIT (1947).

4. Goring, G. E., "Effect of Pressure on the Rate of CO_2 Reduction by High Temperature Coke in a Fluidized Bed", Sc.D. Thesis, Chem. Eng., MIT (1949).

5. Oshima, Y., and Fukuda, Y., Fuel in Sc. and Pract. Vol. XI, 4, 135 (1932).

6. Langmuir, I., J. Am. Chem. Soc., 38, 2221 (1916).

7. Langmuir, I., J. Am. Chem. Soc., 37, 1154-1156 (1915).

8. Semechkova, A. F. and Frank-Kamenetzky, D. A., Acta Physicochim., U.R.S.S., 12, 879 (1940).

9. deBoer, H. J., "Advances in Catalysis", Academic Press, Vol. VIII, 139 (1956).

10. ibid Vol. IX, 472 (1957).

11. Redmond, J. P. and Walker Jr., P. L., J. Phys. Chem., 64, 1093 (1960).

12. Trapnul, B.M.W.,"Chemisorption", Academic Press, 104, 124 (1955).

13. Temkin, M. and Pyzhev, J., Acta Physicochim. U.S.S.R., 12, 327 (1940).

14. Frumkin, A. and Slygin, A., Acta Physicochim., U.S.S.R., 3, 791, (1935).

15. Zeldowitsch, J., Acta Physicochim., U.S.S.R., 1, 961 (1934).

16. Hinshelwood, C. N., Gadsby, J., and Sykes, K. W., Proc. Roy. Soc., No. 1009, Vol. 187, 129-151 (1946).

17. Leinroth, Jr., J. P. and Duffy, Jr., B. J., "The Rate of Gasification of Anthracite Coke by Carbon Dioxide in a Fluidized Bed", S. M. Thesis, Chem. Eng., MIT (1947).

Reduction of Incendivity of Hot Gases to Methane and Coal Dust

J. M. Singer,[1] N. E. Hanna,[2] R. W. Van Dolah,[3] and J. Grumer[4]

Bureau of Mines, Pittsburgh, Pennsylvania

ABSTRACT

Hot gases produced by explosives are known to constitute a possible ignition hazard in coal mines. Experiments in the large test gallery of the Bureau of Mines have established that sodium chloride reduces the incendivity of explosives. In the present investigation the effect of sodium nitrate was explored. This study was conducted in two phases. Gallery experiments showed that sodium nitrate reduced the incendivity of certain explosives to 8 percent natural gas in air, but increased their incendivity to coal dust predispersed in air. Laboratory experiments using hot jets from explosions of stoichiometric mixtures of methane-oxygen-nitrogen showed that both sodium chloride and sodium nitrate reduced the incendivity to methane, to mixtures of coal dust and methane, and to coal dust. The difference between the gallery and laboratory results with respect to coal dust is attributed to temperature-time effects. In the gallery experiments, the sodium nitrate probably forms sodium oxide which affects the incendivity of the hot gases. In the hot jet case, it is possible that the nitrate is not as completely decomposed and has a different effect on incendivity.

INTRODUCTION

The hot gases produced by explosives constitute a possible ignition hazard in coal mines. Components of explosives known to affect incendivity of explosives are sodium nitrate and sodium chloride. Large scale gallery experiments with sodium chloride had confirmed that it reduces the incendivity of explosives,[5] but the effect of sodium nitrate had not been systematically explored. As sodium nitrate is an oxidant, it was conceivable that it might increase the incendivity of explosives to methane or coal dust dispersed in air. On the other hand it might have an inhibiting action similar to that of sodium chloride. The present study sought to determine whether sodium nitrate inhibits or promotes the ignition of mixtures of methane, coal dust, or both with air.

In one phase of this study, an investigation was conducted in a gallery 6-1/3 feet in diameter, with a 20 foot long section filled with 8 percent natural gas or coal dust predispersed in air. Concentrations of coal dust in air were about 300 mg/liter. This and the 8 percent natural gas concentration in air are both much higher than the lean flammability limit of the respective fuel. Explosives containing natural and synthetic sodium nitrate were fired in the gallery and their incendivity

---

1/ Research chemist, Explosives Research Center, Bureau of Mines, Pittsburgh, Pa.

2/ Research chemist, Health and Safety Research and Testing Center, Bureau of Mines, Bruceton, Pa.

3/ Research director, Explosives Research Center, Bureau of Mines, Pittsburgh, Pa.

4/ Project coordinator, Flame Dynamics, Explosives Research Center, Bureau of Mines, Pittsburgh, Pa.

5/ Hanna, N. E., G. H. Damon, and R. W. Van Dolah. Probability Studies on the Incendivity of Permissible Explosives Effect of Small Percentages of Sodium Chloride, BuMines Rept. of Inv. 5463, 1959, 22 pp.

was determined by the Bureau's standard up-and-down method.[6] Sodium nitrate reduced the incendivity to methane but increased the incendivity to coal dust. Another phase of the study sought to model gallery conditions through small scale laboratory experiments in which the ignition sources were small pulsed hot gas jets produced by explosions of stoichiometric mixtures of methane-oxygen or such mixtures diluted with nitrogen. These small jets were "salted" or not, so that the relative promoting or inhibiting effect could be determined. The fuel-air mixtures exposed to these jets when not salted were fuel-lean mixtures of methane plus coal dust (hybrid mixtures) or coal dust. Concentrations of coal dust and methane in the hybrid air mixtures were generally below concentrations at their lean flammability limits. The oxygen index [oxygen/(oxygen + nitrogen)] of the ignition source was the index of incendivity. It was used to vary the temperature of the hot jet which increased as the oxygen index was increased. Temperatures of these jets are noted in table 1 along with other characteristics. The ability of the technique to detect changes in incendivity was confirmed by experiments with sodium chloride. Sodium nitrate was found to reduce the incendivity of the hot gases with respect to all three of the fuel systems. This experimental technique should make it possible to survey a large number of ignition inhibitors to select the materials which are most effective in reducing the ignition hazard of hot gases from detonating charges in coal mines.

ACKNOWLEDGEMENT

The authors wish to thank Bituminous Coal Research, Inc., Monroeville, Pa. for furnishing the ultrafine grind of coal dust.

EXPERIMENTAL EQUIPMENT AND PROCEDURE

Gallery Experiments

Equipment used in these experiments were the same as those used to evaluate the permissibility of explosives according to schedule 1-H.[7] The first experiment had a 2 x 3 factorial design and was conducted by firing from a stemmed cannon into 8 percent natural gas-air mixtures (gallery test 7).[7] Its purpose was to compare the six explosive formulations in table 2, which are based on the composition of two different permissible explosives (A and B). The samples based on composition A contained about 4 percent sodium nitrate; those based on composition B contained 10 percent sodium nitrate. Both synthetic (99.5% pure) and natural (98.5% pure) sodium nitrate was used, with the natural in two ranges of particle size. The average particle diameter of the coarse natural, ground natural, and synthetic sodium nitrate was 1,170, 317, and 437 microns, respectively. Each of the six explosives was carried through the up-and-down sequence, varying the weight of explosive to obtain W_{50} values.[8] Ten pairs of ignition-nonignition results were obtained in each up-and-down sequence.

The second experiment was also given a 2 x 3 factorial design to compare the incendivity of the same explosives to coal dust (300 mg/liter) predispersed in air. The coal dust was of Pittsburgh Seam coal; its average particle diameter was 80 microns and the proximate analysis was 2.0 percent moisture, 34.9 percent volatile, 55.4 percent fixed carbon, and 7.6 percent ash. In this experiment, 5.5 kilos of

---

6/ Hanna, N. E., P. A. Richardson, and R. W. Van Dolah. An Improved Method for Evaluating the Incendivity of Explosives to Coal Dust: A Preliminary Report. Restricted International Conference of Directors of Safety in Mines Research, Sheffield, England, 1965, Paper No. 12.

7/ Federal Register, March 1, 1961, v. 26, No. 39. Title 30 - Mineral Resources, Schedule 1-H, p. 1761.

8/ W_{50} is weight of explosive producing 50 percent probability of igniting a natural gas-air atmosphere; W_{50} values increase as incendivity decreases.

Table 1. - Characteristics of hot turbulent gas jets (ignition sources)

Oxygen index [1]	Adiabatic flame temperature, ° K	Observed [2] maximum temperature, ° K	Jet velocity, [3] m/sec	Length [3] of jet, cm
1.0	3050	2740	137	12.8
.75	2975	2650	98	9.0
.50	2813	2480	59	6.4
.35	2620	2270	36	5.4
.30	2510	2510	28	5.0
.26	2400	2020	22	4.7
.21	2200	1820	16	4.3

1/ $O_2/(O_2 + N_2)$ of stoichiometric mixture containing methane.

2/ Experimental values determined by the sodium D line reversal technique.

3/ Velocity of advance of head of jet from orifice. Velocity was constant between time zero and growth of jet to maximum length (point of sharp decrease in luminosity and start of break-up of jet).

Table 2. - Incendivity of products from explosives containing sodium nitrate and sodium chloride

	A formulations			B formulations		
Chemical analysis:						
Moisture	0.3	0.2	0.2	0.4	0.3	0.4
Nitroglycerine	8.8	8.7	8.8	10.6	10.7	10.5
Nitrocellulose	.3	.3	.3	.3	.3	.2
Ammonium nitrate	68.3	67.6	68.1	57.6	57.1	56.9
Sodium nitrate	1/ 3.8	2/ 3.9	3/ 3.8	1/ 10.3	2/ 9.3	3/ 9.9
Sodium chloride	9.2	9.5	9.1	10.4	10.1	9.8
Antacid	.4	.3	.5	.3	.5	.5
C.C.M. 4/	8.9	9.8	9.2	10.1	11.6	11.8
Physical properties:						
Apparent specific gravity	1.06	1.05	1.05	0.84	0.82	0.81
Grams wrapper per 100 g explosive	7.3	7.7	7.3	8.2	8.5	8.5
Ballistic mortar, percent strength of TNT	96	97	96	89	89	90
Rates of detonation, meters per second	2470	2360	2480	2630	2570	2580
Oxygen Balance, grams oxygen per 100g explosive	-11.6	-13.3	-12.5	-15.5	-18.1	-19.1
Incendivity, Gallery Results:						
W_{50}, grams 5/	615	600	590	670	650	670
W_{CD}, grams 6/	300	290	490	80	90	90

1/ Coarse natural nitrate, average particle size 1171 microns.
2/ Fine synthetic nitrate, average particle size 437 microns.
3/ Ground natural nitrate, average particle size 317 microns.
4/ Carbonaceous combustible material.
5/ Weight for 50 percent probability of ignition in 8 percent natural gas-air: stemmed cannon shots.
6/ Weight for 50 percent probability of ignition in predispersed coal dust (300 mg/liter) - air: suspended shots.

coal dust was dispersed in the first section of the gallery 1/2 second before firing an explosive charge suspended in the center of this section which was isolated from the rest of the gallery by a paper diaphragm. The coal dust was spread evenly over a length of 30-grain per foot detonating cord laid in a 20-foot long steel Vee trough made from 6-inch by 6-inch angle and mounted 7 inches above the gallery floor; the detonation of the cord disperses the dust. With this test arrangement, W_{CD} [9/] were determined, again using up-and-down technique.

LABORATORY EXPERIMENTS

The effect of sodium nitrate on incendivity of hot gas jets was investigated using mixtures in air of methane, coal dust, or hybrid mixtures of the two as the acceptor charge. The coal dust was an ultrafine grind (83.5 percent less than 17 microns) of Pittsburgh Seam, Mathies mine coal. The elemental composition in percent by weight was: H_2 = 5.3, C = 78.9, O_2 = 8.0, N_2 = 1.6, S = 1.3, and ash = 4.9. The proximate analysis in percent by weight was: Moisture, 0.7; volatile matter, 37.0; fixed carbon, 57.5; and ash, 4.8. All gases were obtained in cylinders and were chemically pure grade except for air. Sodium chloride and sodium nitrate of chemically pure grade were ground to minus 20 micron particle size.

The hot gas ignition apparatus (figure 1) and coal dust disperser (figure 2) have been described earlier.[10/] The explosion vessel consists of two chambers, one

---

Figure 1. - Hot Gas Ignition Apparatus.

Figure 2. - Coal Dust Disperser.

---

partially within the other (figure 1). The small chamber A (76 cc) was capped and communicated with the large chamber B (2.1 liters) through a straight channel, 0.5 cm in diameter and 1.0 cm long. After purging and filling chamber A with a stoichiometric methane-oxygen-nitrogen mixture, the cap was removed and the contents were spark-ignited near the channel opening. The explosion products vented through the channel into the flammable mixture in chamber B. These jets differed in temperatures as shown in table 1, both by their calculated theoretical temperatures assuming adiabatic combustion, and by measured temperatures using the sodium D line reversal technique. Natural gas used in these experiments contained about 91 percent methane and 6 percent ethane. Chamber B was equipped with top plates having an array of small venting holes, a blowout pressure release diaphragm at the sidewall, and viewing windows. The outer face of the diaphragm was inerted with nitrogen to eliminate spurious luminosity due to secondary combustion in surrounding air of the hot, partially burned explosion products. The premixed coal dust-methane-air mixture to be ignited flowed through chamber B at approximately 140 cc/sec, giving a constant average linear upward speed of 2.2 cm/sec.

In determining an ignition limit, the coal dust concentration was held constant and the methane concentration was increased until ignition occurred. The salt being investigated for its inhibiting or promoting action was added to chamber A prior to spark ignition by mechanically vibrating the duster (figure 1, view C) that had previously been filled with the requisite amount of additive. Amounts placed in

---

9/ W_{CD} is the weight of explosive producing 50 percent probability of igniting a coal dust atmosphere. W_{CD} values increase as incendivity decreases.

10/ Singer, J. M. Ignition of Mixtures of Coal Dust, Methane and Air by Hot Laminar Nitrogen Jets. Ninth International Symposium on Combustion, 1963, Academic Press, Inc., New York, N. Y., pp. 407-414.
Singer, J. M. Ignition of Coal Dust-Methane-Air Mixtures by Hot Turbulent Gas. BuMines Rept. of Inv. 6369, 1964, 24 pp.

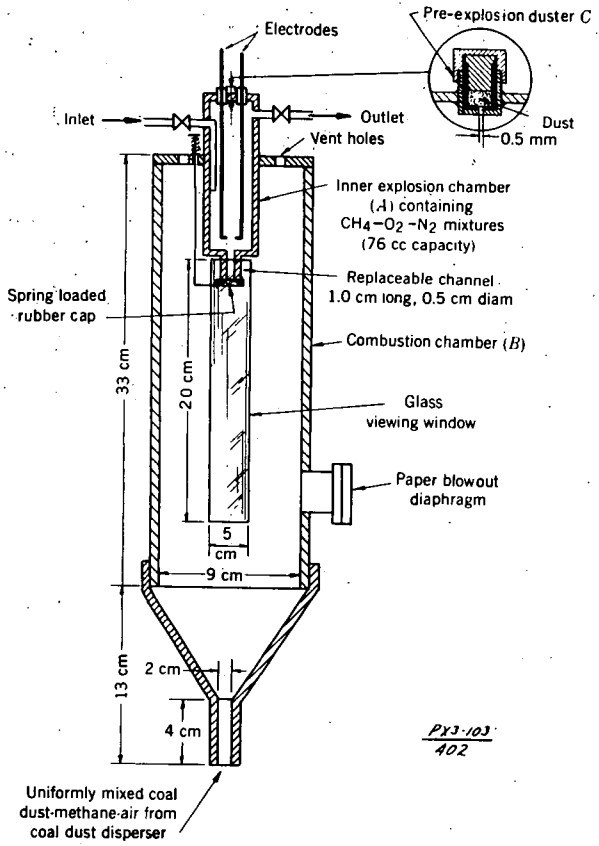

Figure 1. - Hot Gas Ignition Apparatus.

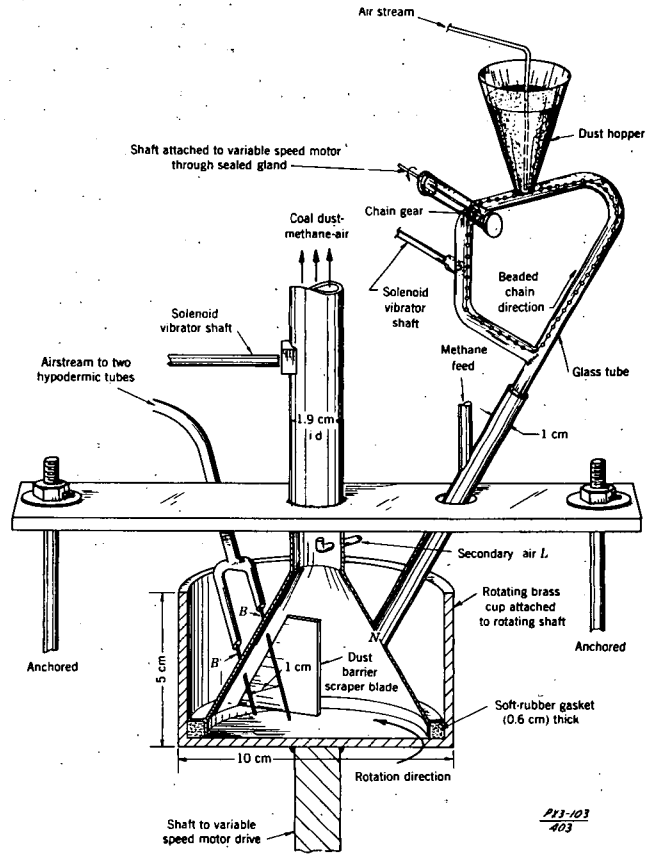

Figure 2. - Coal Dust Disperser.

chamber A are stated in figure 3. The actual amount of additive entrained by the

Figure 3. - Effects of sodium salts on incendivity of hot jets to methane-coal dust-air mixtures.

hot jet is not known. The criteria of ignition after the hot jet entered chamber B was the luminosity observed throughout B, and the simultaneous luminous flame shooting out of the ruptured pressure release diaphragm. Duplicate runs made at each ignition point showed that methane-in-air concentrations were reproducible to 0.15 percentage units, oxygen indices to within 0.02 units and coal dust concentrations to within 20 percent. Coal dust concentrations were determined on separate runs by filtering the entire mixture at different levels of chamber B through a 4 cm diameter glass-wool cartridge and weighing after a selected time interval. Local concentrations of dust were determined by filtering through a paper extraction thimble on a 1.0 cm diameter iso-kinetic sampling probe. Local concentrations of dust at various heights and radii of chamber B were constant to within 20 percent. Concentrations of fuel in chamber B at the ignition limit are termed "lower ignition limits", and correspond to lower flammability limits, except that ignition limits are dependent on apparatus factors.

The coal dust disperser in figure 2 was continuously fed by an endless beaded-chain carrier that removed dust from the hopper at a rate determined by its rotation speed. Methane was added through an inlet to the dust disperser. Not all of the air could be added through the air jets; the balance was added through duct L. Hypodermic needles, dust carrier tubes, and chamber B were continuously vibrated to facilitate dust movement and to prevent dust deposition.

RESULTS AND DISCUSSION

Gallery Experiments

The W_{50} values obtained for the six samples are given in table 2. The values for the three explosives containing the low percentage of sodium nitrate varied from 590 to 615 grams; and the values of the three high sodium nitrate explosives varied from 650 to 670 grams. A statistical analysis of these data showed that the type and fineness of the sodium nitrate had no significant effect on the incendivity of the explosives to natural gas air mixtures. However, the samples with the high sodium nitrate content were consistently less incendive than those with low sodium nitrate concentrations.

The W_{CD} values for the low sodium nitrate explosives (a) formulation varied from 290 to 490 grams; the W_{CD} values for the high sodium nitrate explosives (b) formulations varied from 80 to 90 grams. As in the previous experiment the type and fineness of the sodium nitrate does not appear to have any significant effect on the incendivity to coal dust. The 10 percent sodium nitrate explosives were more incendive in coal dust-air atmospheres than the 4 percent sodium nitrate explosives. The reverse was the case for natural gas-air, but differences were much smaller.

The concentration of other constituents of the explosives were changed; nitroglycerin increased about 17 percent between A and B formulations, ammonium nitrate decreased by 18 percent, sodium chloride increased by 10 percent and the combustible carbonaceous matter increased by 19 percent. The sodium nitrate increase was much greater, being about 155 percent. The net result of these changes in chemical composition is that the oxygen balance is more negative for the B formulations than for the A group of explosives. (The oxygen balance is the deficiency or excess of oxygen required for stoichiometric explosion, in units of grams of oxygen per 100 grams of explosive.) Problems of interpretation due to changes in composition other than changes in sodium nitrate concentration will be discussed later.

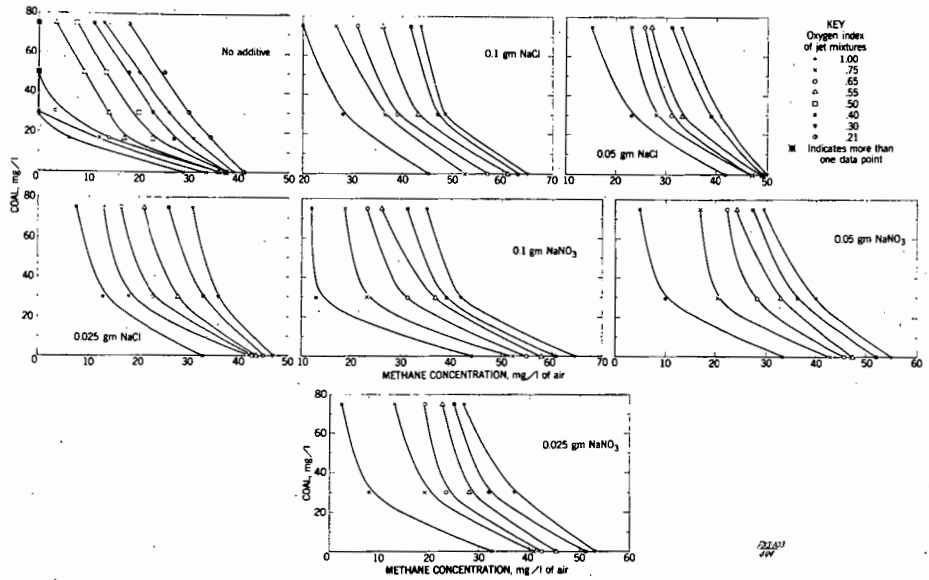

Figure 3. - Effects of Sodium Salts on Incendivity of Hot Jets to Methane-Coal Dust-Air Mixtures.

Laboratory Experiments

Lower ignition limits with and without sodium nitrate in the hot gas jet which served as an ignition source are shown in figure 3; no ignition is obtainable to the left of any curve with the jet used. Each jet is characterized by its oxygen index. The fuel-air mixtures subjected to these jets range from methane-air (lean limit of flammability for methane, 35 mg/liter) to hybrid mixtures of methane-coal dust-air to coal dust-air mixtures (stoichiometric concentration of coal dust used, 109 mg/liter). As the incendivity of the hot jet is decreased by decreasing the oxygen index or adding sodium salts, the lower ignition limits are displaced upward for constant methane concentration and to the right for constant coal dust concentration. Table 3 gives the reduction in incendivity as measured by an increase in oxygen index of the jet required to ignite a given fuel mixture; the composition of the fuel mixture is given in terms of concentrations of methane and coal dust. Table 4 summarizes in another way, the change in incendivity due to the sodium salts. As the incendivity of the jet decreases due to the salts (comparisons for constant oxygen index and coal concentrations) more methane must be added to the fuel mixture to keep it ignitible. The increase in methane is indicated in table 4 by the increase in total fuel concentration.

The data for sodium chloride shows that the hot jet technique is capable of demonstrating the known effectiveness of sodium chloride in reducing incendivity.[5/] The data for sodium nitrate parallel the trend of the sodium chloride data, but at a lesser level of effectiveness. Both salts reduce incendivity of the hot jet toward methane, a hybrid mixture of methane and coal dust or coal dust only. This result was not the case in the gallery experiments in which sodium chloride reduced incendivity to gas and to coal dust, but sodium nitrate only reduced incendivity to gas while increasing incendivity to coal dust.

It is difficult, without further investigation, to pinpoint the reason for the difference in the two sets of results. The gallery determinations were done with coal dust concentrations of 300 mg/liter in air, and the average particle diameter of the coal dust was 80 microns. The coal dust used in the hot jet determinations was of a much finer grind; concentrations used were below 80 mg/liter. It is not known whether these differences would lead to any specific chemical effect between coal dust and sodium nitrate. There are also differences between the two sets of formulations of the explosives (table 2). The overall changes in stoichiometry between formulations A and B resulted in more combustible materials being present in the products of explosion of the B formulation than in those of the other. Perhaps secondary burning in air may have contributed to the greater incendivity of the B formulations, rather than the greater concentration of sodium nitrate. However, afterburning of the richer fuel concentration in the explosion products should increase incendivity to natural gas as well as to coal dust unless the ignitibility of coal dust is far more dependent than gas on the temperature of the ignition source.[11/]

The striking difference in the two experiments may be due to the condition of the sodium nitrate when the hot gases are injected into the fuel-air mixture. In the case of the gallery experiments, the nitrate may be completely reacted with fuel materials in the detonation front or shortly thereafter. A usually assumed product of its reaction is sodium oxide. In the hot jet experiment it is possible that less sodium oxide is formed in the time available. Thus the possibility exists that sodium compounds derived either from sodium chloride or sodium nitrate in the detonation gases may be a specific inhibitor for the ignition of methane, and that sodium oxide may have a specific ignition promoting mechanism for coal dust. In the hot jet case, sodium chloride and sodium nitrate may play essentially equal roles.

11/ Singer, J. M. and J. Grumer. Equivalences of Coal Dust and Methane at the Lower Ignition Limits of Their Mixtures. Restricted International Conference of Directors of Safety in Mines Research, Sheffield, England, 1965, Paper 13, 22 pp.

Table 3. - Incendivity of hot gas jets: minimum oxygen indices of jets required to ignite coal dust-methane-air mixtures.

Fuel Compositions		Additives in ignition jet[1]						
Coal dust Concentration, mg/liter	Methane Concentration, mg/liter	No additive	0.1 gm NaCl	0.1 gm $NaNO_3$	0.05 gm NaCl	0.05 gm $NaNO_3$	0.025 gm NaCl	0.025 gm $NaNO_3$
0	35	0.54	n[2]	n	n	0.95	0.94	0.94
	40	.23	n	n	n	.80	.80	.77
	45	.21	n	1.0	0.88	.65	.44	.55
	50	.21	0.86	.81	.30	.50	.21	.40
30	0	.75	n	n	n	n	n	n
	10	.60	n	n	n	1.0	n	0.9
	20	.50	n	0.80	1.0	.75	0.70	.70
	30	.21	0.90	.60	.70	.65	.50	.50
	40	.21	.65	.38	.35	.30	.26	.30
50	0	.65	n	n	n	n	n	n
	10	.55	n	n	n	0.9	1.0	0.85
	20	.30	n	0.80	1.0	.73	.65	.65
	30	.21	0.80	.60	.55	.53	.40	.35
	40	.21	.55	.26	.26	.30	.21	.21
75	0	.60	n	n	n	n	n	n
	10	.45	n	n	n	0.85	0.85	0.80
	20	.21	1.0	0.73	0.88	.70	.70	.65
	30	.21	.70	.45	.45	.30	.35	.30
	40	.21	.45	.21	.21	.21	.21	.21

1/ Weight of additive in primary chamber before ignition.
2/ n = Not ignitible with oxygen index of unity.

Table 4. - Total concentrations[1] of coal dust and methane at the lower ignition limits of their mixtures with and without the additives sodium chloride and sodium nitrate

Additives in ignition jet[2]	None			0.1g NaCl			0.1g $NaNO_3$			0.05g NaCl			0.05g $NaNO_3$			0.025g NaCl			0.025g $NaNO_3$		
Oxygen index of jet	1.0	0.55	0.3	1.0	0.55	0.3	1.0	0.55	0.3	1.0	0.55	0.3	1.0	0.55	0.3	1.0	0.55	0.3	1.0	0.55	0.3
Coal dust concentration, mg/l:																					
0	0.45	0.55	0.59	0.68	0.92	0.95	0.68	0.88	0.95	0.62	0.71	0.72	0.52	0.71	0.80	0.50	0.65	0.70	0.50	0.69	0.79
30	.30	.46	.65	.68	.90	.96	.48	.82	.89	.60	.75	.86	.42	.75	.82	.48	.68	.81	.40	.68	.83
50	.45	.58	.75	.80	1.03	1.12	.62	.93	1.02	.73	.92	1.0	.53	.91	.99	.53	.83	.95	.50	.83	.93
75	.65	.70	.85	.94	1.13	1.27	.80	.98	1.15	.90	.98	1.1	.72	.95	1.01	.70	.94	1.02	.65	.95	.98

1/ Fraction of stoichiometry of coal dust-methane-air for complete combustion.
2/ Weight of additive in primary chamber before ignition.

The effect of additives on ignition has been examined recently by several investigators. The experiments of Singer using hot laminar nitrogen jets[12/] and hot pulsed jets[13/] as ignition sources indicated that (1) gaseous inhibitors were more effective when added to hot laminar nitrogen jets than to the fuel mixtures to be ignited, and (2) inhibitors suppressed ignition by hot pulsed turbulent jets less efficiently than ignition by hot continuous laminar jets. In ignition by hot pulsed turbulent jets, higher temperatures and high rates of heat and mass transfer to the dust mixtures nullified the effect of the volatile inhibitors. In hot continuous laminar jets, the same compounds were powerful ignition suppressors, apparently because they inhibited slow chemical reactions coupled to the slow diffusion of oxygen and fuel into the slower moving hot gases.

Most of the work reported by other investigators[14/] concerns suppression of flames of gas mixtures by well-known inhibitors such as halogenated hydrocarbons and alkali metal compounds. Flame inhibition mechanisms suggested for gas mixtures usually relate the condition that chain branching of the active species will equal chain breaking in flames of mixtures with a minimum (or zero) flame velocity or in flames at the upper and lower flammability limits. Dust inhibitors are presumed to act either as coolants or as chemical inhibitors attacking free radicals responsible for chain reaction. One explanation is that the efficiency of a chemical inhibitor is related to the ease of removal of a free valence electron by a colliding radical. Sodium nitrate and sodium chloride are classed as both thermal and chemical inhibitors.

12/ First work cited in footnote 10.

13/ Second work cited in footnote 10.

14/ Abrams, M. C. Chemical Flame Quenching Theory. Pyrodynamics, v. 1, 1964, pp. 131-141.

Dewitte, M., J. Vrebosch, and A. Van Tiggelen. Inhibition and Extinction of Premixed Flames by Dust Particles. Combustion and Flame, v. 8, No. 4, Dec. 1964, pp. 257-266.

Dolan, J. E. The Suppression of Methane/Air Ignitions by Fine Powders. Sixth Symposium (International) on Combustion, Reinhold Publishing Co., New York, pp. 787-794.

Dolan, J. E. and J. B. Dempster. The Suppression of Methane-Air Ignitions by Fine Powers, J. Appl. Chem. v. 5, 1958, pp. 510-517.

Rosser, W. A., S. H. Inami, and H. Wise. The Effect of Metal Salts on Premixed Hydrocarbon-Air Flames, Combustion and Flame, v. 7, June 1963, pp. 107-119.

Van Tiggelen, A. University of Louvian, Final Technical Report on Contract DA-91-591-EUC-1072, March 1960.

CONCLUSIONS

1. The incendivity to methane or natural gas-air mixtures was reduced by the presence of sodium nitrate in explosives or in hot jets from methane-oxygen-nitrogen explosions.

2. The incendivity to methane-coal dust-air mixtures was reduced by sodium nitrate in the hot jets.

3. The incendivity to coal dust was increased by sodium nitrate in explosives and decreased by sodium nitrate in the hot jets.

AN ANALYSIS OF POROUS-PLATE COMBUSTION SYSTEMS

by

S. A. Weil
W. R. Staats
R. B. Rosenberg

Institute of Gas Technology
Chicago, Illinois

INTRODUCTION

In the porous-plate combustion system, an unburned gaseous fuel-oxidant mixture is fed into the upstream side of a porous solid. The combustion or reaction zone is near the downstream surface. The variety of possible pore structures and solid materials offers a variety of reaction areas. They include combustion in the gas phase above the solid (a flame), in pores large enough to permit essentially ordinary flames, in pores too small to permit ordinary flames, on the pore surfaces within a catalytic porous medium, and combinations of these.

This paper presents a theoretical analysis of combustion in and above a noncatalytic solid with fine pores. Its purpose is to indicate the limits of steady-state operation of such a system, and the operating characteristics as they depend on flow rate.

The location of the combustion zone is deduced from the model, rather than included in the assumptions. Potentially, the porous plate can operate either as a preheater or as a reactor. In the first case, the incoming gases are heated in the plate and most of the combustion occurs above it. In the other case, most of the combustion occurs in the plate. The characteristics of both mechanisms are of interest here. The quantitative results are necessarily inseparable from the assumed chemical kinetics and physical properties. These have been chosen to correspond to reasonably real systems, but in any case, they demonstrate the types of operating boundaries to be encountered in such systems.

THE HYPOTHETICAL MODEL

The system is defined to be unidimensional, with a semi-infinite porous solid. Within the porous phase, the gas and solid temperatures are equivalent, and the pores are sufficiently fine that the equations applicable to a homogeneous phase can be used. The chemical kinetics are the same within the pores as in the gas phase outside the solid.

The equations to describe the energy and mass transfer in this system are based on those presented by Spalding.[1] To solve the equations, even numerically, a relationship between the local temperature and composition is extremely convenient. In the porous phase, the assumption of no mass diffusion generates this relationship. In the gas region, the assumption of a Lewis number of 1, as originally suggested by Semenov,[2] serves this purpose.

Furthermore, the formulation of the overall kinetics of the reaction is most conveniently set in terms of mass fraction of the fuel (for a lean system) and the temperature, in the manner used by Spalding.[3] The resulting steady-state equations, in terms of reduced variables, are:

For the region outside the solid

$$d^2\tau/dy^2 - d\tau/dy + a^n\tau^m/g^2\lambda^2 = 0 \qquad (1)$$

$$\alpha = \tau_f - \tau \tag{2}$$

For the porous region

$$r_k d^2\tau/dy^2 - d\tau/dy + \alpha^n \tau^m P/g^2\lambda^2 = 0 \tag{3}$$

$$\alpha = 1 - \tau + r_k \, d\tau/dy \tag{4}$$

where

τ = temperature above the feed gas temperature relative to the adiabatic temperature rise

y = distance × gas specific heat × gas mass velocity / gas thermal conductivity

α = fuel mass fraction relative to inlet fuel mass fraction

r_k = mean solid thermal conductivity relative to that of the gas

g = mass velocity relative to the adiabatic burning velocity

n = overall order of reaction in terms of fuel fraction

τ^m = temperature dependence of reaction rate

P = porosity of the solid

λ^2 = constant

The interaction of the system with the surroundings occurs only by radiation to and from the porous-plate surface. With this, the conditions at the boundaries are:

$$y = -\infty: \quad \tau = 0, \quad d\tau/dy = 0 \tag{5}$$

$$y = \infty: \quad \tau = \tau_f, \quad d\tau/dy = 0 \tag{6}$$

$$y = 0: \quad \epsilon\tau^s = g(1 - \tau_f) + \epsilon\tau_b^s \tag{7}$$

$$\tau_f = 1 + r_k (d\tau/dy)_{y<o} - (d\tau/dy)_{y>o} \tag{8}$$

if y is zero at the surface, τ_f is the final gas temperature, τ_b is the temperature of the surroundings, and $\epsilon\tau^s$ is the radiation law for the solid.

The solution of Equations 1 through 8 for a specified g and τ_b consists of finding a temperature distribution in the porous phase from 3 and 5, and one in the gas phase from 1 and 6, that can be linked up at the surface in accordance with 7 and 8. Two, one, or no solutions may exist, for a given flow rate and surrounding temperature, depending on the operating parameters.

Although reaction occurs in both phases, the solutions correspond to the porous phase acting primarily as a heater, with the major combustion in the gas phase, or to the major combustion occurring in the porous phase. In this paper, these regimes are referred to as preheater and reactor, respectively, to emphasize the role of the porous solid.

The lack of a steady-state solution must imply the impossibility of stable operation for the particular input and surrounding temperature. Also, more than one steady-state solution may exist for any given set of conditions. On the other hand, the existence of a steady-state solution does not necessitate stable operation, since other factors may be involved.

RESULTS

In the primary example used for analysis, values of the parameters are $n=2$, $m=10$, $\epsilon=1.17$, $S=3$ and $P=0.3$. As shown in previous work,[3] $m=10$ is appropriate for methane-air systems. For a 105 percent aerated flame with an adiabatic flame temperature of 2190°K, the values for ϵ and S correspond to a black-body radiation law. Two values of r_k were studied, 5 and 20, corresponding to insulating and high-conductivity porous solids, respectively.

In Figure 1, a typical set of temperature distribution curves is presented. Note that Equations 3, 4, and 5 define the temperature distribution in the porous phase with the flow rate as the only operating parameter. The maximum τ increases monotonically with flow rate. Any finite flow rate will yield a porous phase steady-state solution. However, the whole system has a valid steady-state solution only if a surface consistent with Equations 6, 7, and 8 exists. The location of the surface with respect to the temperature distribution of the porous phase depends on the surrounding temperature and on the solution for the gas phase.

In Figure 2, the steady states for a surroundings temperature (τ_b) of 0.4 are shown for $r_k = 5$ in terms of the surface and final gas temperatures. This is the behavior of these systems when τ_b is low. The lower input limit is the same for the solid behaving as a reactor or as a preheater. It is not zero if τ_b is greater than zero. The upper input limit of the preheater region corresponds to the situation when all the incoming radiation goes into preheating the gas. Another notable characteristic is the maximum in the surface temperature vs. feed rate curve for preheater operation. Thus, a maximum yield of radiation energy exists for this type of operation.

The choice when there are two possible steady states at a given flow rate presumably is determined by the path to the steady state. If the burner is started cold at a flow rate within the preheat region, it will behave as a preheater. If it is started at a higher rate where the solid is a reactor, a reduction in flow rate would keep the system in that regime. The type of instability which results from a reduction of the flow rate beyond the lower input limit is not known from this analysis. However, the extent of reaction is 46 percent within the solid at the lower limit, which would indicate that the system would go into flashback.

In Figure 3, the characteristics of the same system ($r_k = 5$) at high surrounding temperatures are illustrated with $\tau_b = .6$. At low flows, no steady states are possible. The regimes, in order of increasing flow rate, then consist of one in which only preheater behavior is possible, one in which both preheater and reactor behavior is possible, and one in which only reactor behavior is possible. These results imply the existence of two lower limits, depending on operation as a preheater or as a reactor. Again, this type of analysis cannot anticipate the behavior at these bounds, in particular whether the lower limit for the reactor corresponds to a discontinuous transition to preheater behavior or directly to flashback.

The equivalent system, but with a higher relative thermal conductivity for the porous phase, $r_k = 20$, is similar to the $r_k = 5$ system in most aspects. The separation of the lower bounds for preheater and reactor occurs at lower surrounding temperatures, as shown in Figure 4. At higher temperatures, another type of behavior appears. For $\tau_b = 0.6$, (Figure 5) there is a flow region too high for preheater activity and too low for reactor behavior.

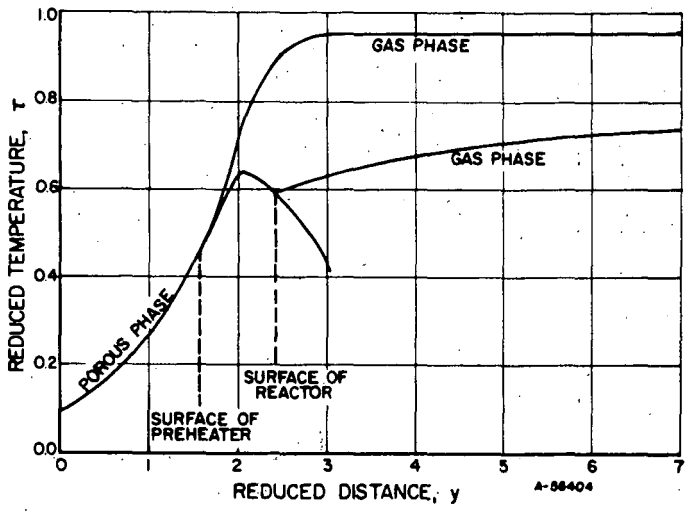

Fig. 1.–TEMPERATURE DISTRIBUTIONS IN POROUS SOLID AND GAS PHASES WITH POROUS PHASE ACTING AS PREHEATER AND AS REACTOR, $\tau_b = 0.4$, $r_k = 5$.

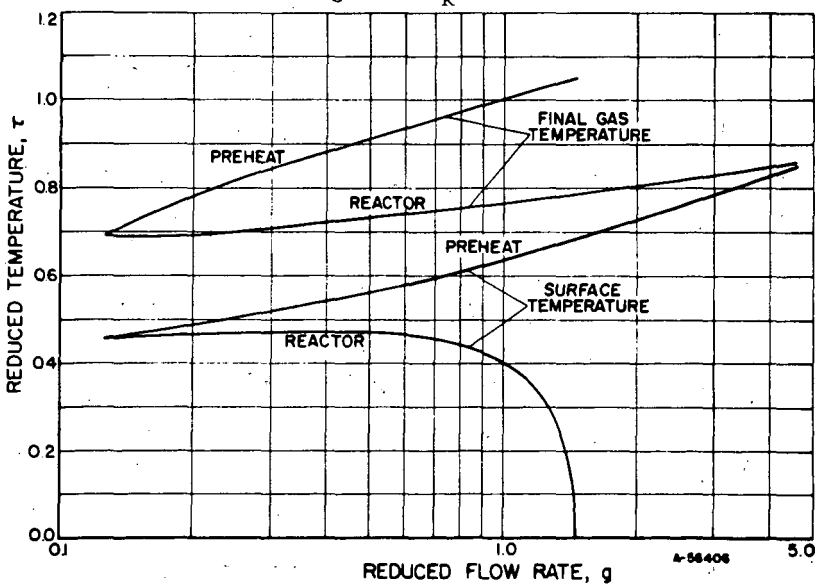

Fig. 2.–FINAL GAS TEMPERATURE AND TEMPERATURE OF THE SURFACE OF THE POROUS SOLID AS FUNCTIONS OF GAS FLOW RATE, $\tau_b = 0.4$, $r_k = 5$.

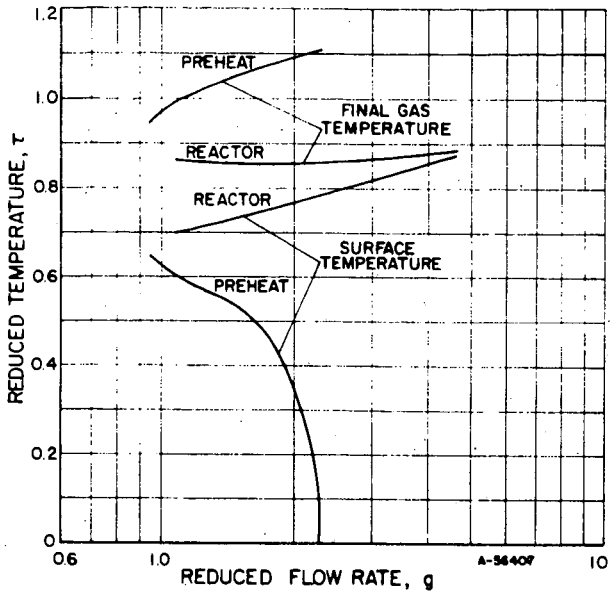

Fig. 3.–FINAL GAS TEMPERATURE AND TEMPERATURE OF THE SURFACE OF THE POROUS SOLID AS FUNCTIONS OF FLOW RATE, $\tau_b = 0.6$, $r_k = 5$.

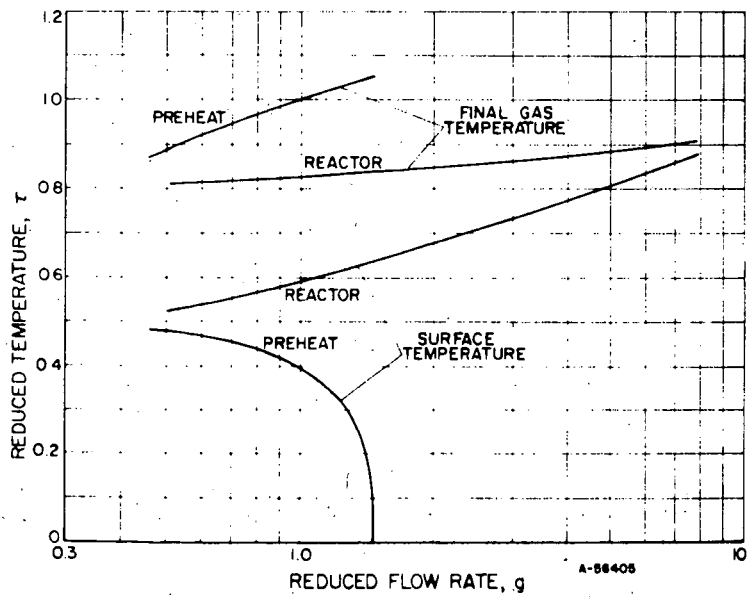

Fig. 4.–FINAL GAS TEMPERATURE AND TEMPERATURE OF THE SURFACE OF THE POROUS SOLID AS FUNCTIONS OF GAS FLOW RATE, $\tau_b = 0.4$, $r_k = 20$.

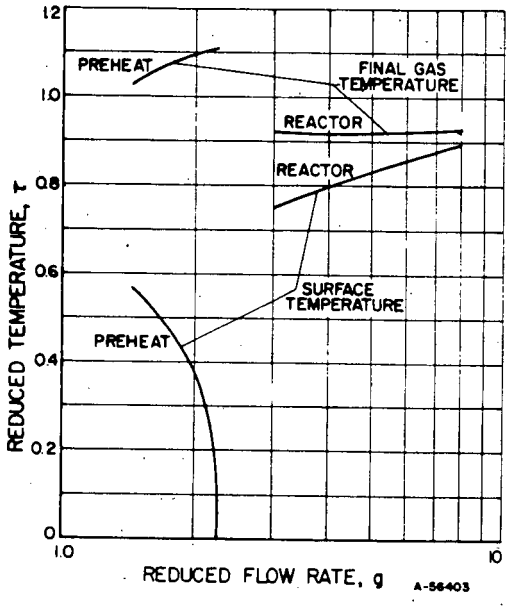

Fig. 5.—FINAL GAS TEMPERATURE AND TEMPERATURE OF THE SURFACE OF THE POROUS SOLID AS FUNCTIONS OF GAS FLOW RATE, $\tau_b = 0.6$, $r_k = 20$.

SUMMARY

The theoretical analysis demonstrates the existence of heat input limits (limits of steady-state operation) for a noncatalytic porous-plate burner. It indicates the relative location of these limits and the effect of the temperature of the surroundings. The analysis also shows the surface temperatures as a function of input and surrounding temperature.

The porous plate can operate in two ways:

1) As a preheater — The incoming gases are preheated as they pass through the plate, with most of the combustion occurring above the plate.

2) As a reactor — The fuel-air mixture reacts primarily in the plate rather than above it.

Three different input limits for steady-state operation are shown to exist:

1) An upper limit for operation as a preheater.

2) A lower limit for preheater operation.

3) A lower limit for reactor operation.

Limits 2 and 3 can be identical under some conditions.

The porous plate can sometimes act either as a preheater or as a reactor at a given input. In such a case, it may be difficult to visually differentiate between the two mechanisms since the plate surface temperatures are often similar. The appropriate mechanism can be determined most readily by determining the effect of variations in the input rate on the surface temperature.

REFERENCES CITED

1. Spalding, D. B., "II. One-Dimensional Laminar Flame Theory for Temperature — Explicit Reaction Rates," Combustion and Flame 1, 296-306 (1957) September.

2. Semenov, N. N. "Thermal Theory of Combustion and Explosion. III. — Theory of Normal Flame Propagation," NACA Technical Memorandum No. 1026 (1942) September.

3. Weil, S. A., "A Study of Porous Plate Flameholders," Institute of Gas Technology Research Bulletin No. 35 (1964) August.

FORMATION OF NITROGEN OXIDES IN AERATED METHANE FLAMES

R. B. Rosenberg and D. S. Hacker

Institute of Gas Technology, Chicago, Illinois

INTRODUCTION

An investigation to determine the kinetics of the formation of the oxides of nitrogen produced in aerated methane flames is currently in progress at IGT. Under controlled flow conditions, the location and concentration of the oxides of nitrogen – nitric oxide, NO, and nitrogen dioxide, NO_2 – were experimentally measured in a premixed bunsen-type flame and on a premixed flat flame. The compositions of the primary stream (fuel-oxidant) and the secondary stream were varied. This paper summarizes the highlights of the work to date. The study is sponsored by the American Gas Association under its PAR (Promotion-Advertising-Research) Plan.

EXPERIMENTAL TECHNIQUE

The data on NO_2 were obtained with a Mast nitrogen dioxide analyzer. The concentrations of NO were initially determined by use of a catalytic probe which converted the NO to NO_2 for later analysis with the Mast. The NO concentrations are currently being obtained by homogeneously oxidizing the NO to NO_2 with oxygen at high pressure prior to analysis. Spot checks by the phenyldisulfonic acid technique are made on the concentration of oxides of nitrogen in the water condensed from the flue gas sample stream. These have not shown significant quantities of nitrogen oxides in most cases.

The reproducibility of the data is very good for runs made on the same day. The worst variations observed for runs on different days were about ±2 ppm. Most of the data showed smaller variations than this.

EXPERIMENTAL RESULTS

Figure 1 shows a bunsen flame which had a primary feed stream consisting of methane with 67 percent of the stoichiometric air required for complete combustion, and a secondary feed stream of air. Figure 2 shows the concentrations of NO and NO_2 measured at various positions in this flame. It can be seen that NO forms in a narrow region near the outside edge of the flame. It then diffuses both toward the center of the burner and into the secondary air stream. It oxidizes rapidly to NO_2 in the secondary air stream. Very little NO_2 is found in the burning gas.

Table 1 shows the average concentration of NO + NO_2 (NO_x) at each height above the burner. This average value corresponds to the concentration of NO_x which would have to be uniformly distributed over the cylindrical cross-section to yield the same total concentration shown at each height in Figure 2. Table 1 shows that the formation of NO_x occurs only where the flame is present. Above the tip of the flame, i.e., at heights greater than 7.2 cm, the concentration is seen to remain constant within experimental uncertainty. This suggests that the flame is acting as more than a source of heat, and may be participating chemically in the formation of NO_x.

Table 1.—AVERAGE NO_x CONCENTRATION AT VARIOUS HEIGHTS ABOVE FLAMEHOLDER WITH A CONICAL FLAME OF 67+ PRIMARY AERATION
(Primary Flow Rate 15.6 CF/hr)

Height Above Flameholder, cm	Average NO_x Concentration, ppm	
	Corrected for Temperature Profile	Uncorrected
0.5	--	1.3
1.8	--	1.7
3.7	3.6	2.9
7.2	4.8	4.5
9.7	--	3.9
15	4.5	4.2

Figure 3 shows the results obtained when argon was substituted for nitrogen in the primary stream, with air retained as the secondary stream. The concentration of argon was varied so that the difference between the heat capacities of argon and nitrogen would not be a factor. The data show a lower concentration of NO_x when argon is substituted for nitrogen. Thus, it is seen that the nitrogen which reacts to form NO_x is supplied by both the primary and secondary streams, with somewhat more being supplied by the secondary.

Tables 2 and 3 show the effect of primary mixture flow rate (heat input) and of primary aeration on NO_x concentration at a height of 15 cm above the burner. The

Table 2.—EFFECT OF PRIMARY MIXTURE FLOW RATE (67% PRIMARY AIR) ON THE CONCENTRATION OF NO_x 15 cm ABOVE FLAMEHOLDER

Primary Mixture Flow Rate, CF/hr	NO_x at Various Radial Positions, ppm		
	0.0 cm	1.2 cm	2.4 cm
12.1	2.7	4.1	3.7
15.6*	3.1 ± 1.0	4.5 ± 0.9	3.5 ± 0.5
20.0	3.5	4.2	3.6
25.0†	1.2 ± 0.5	5.7 ± 0.3	4.8 ± 0.1

* Average of 4 runs † Average of 2 runs

Table 3.—EFFECT OF PRIMARY AERATION ON THE CONCENTRATION OF NO_x 15 cm Above Flameholder

Primary Aeration,	Primary Mixture Flow Rate, CF/hr	NO_x at Various Radial Positions, ppm		
		0.0 cm	1.2 cm	2.4 cm
67.3*	15.6	3.1 ± 1.0	4.5 ± 0.9	3.5 ± 0.5
67.3	20.0	3.5	4.2	3.6
80.0	18.2	1.9	4.4	3.4
67.3†	25.0	1.2 ± 0.5	5.7 ± 0.3	4.8 ± 0.1
90.0†	30.0	4.8 ± 1.1	5.1 ± 0.5	5.4 ± 0.4
110.0†	29.1	3.1 ± 0.1	2.8 ± 0.2	3.0 ± 0.2
120.0	26.3	1.2	1.7	1.9

* Average of 4 runs † Average of 2 runs

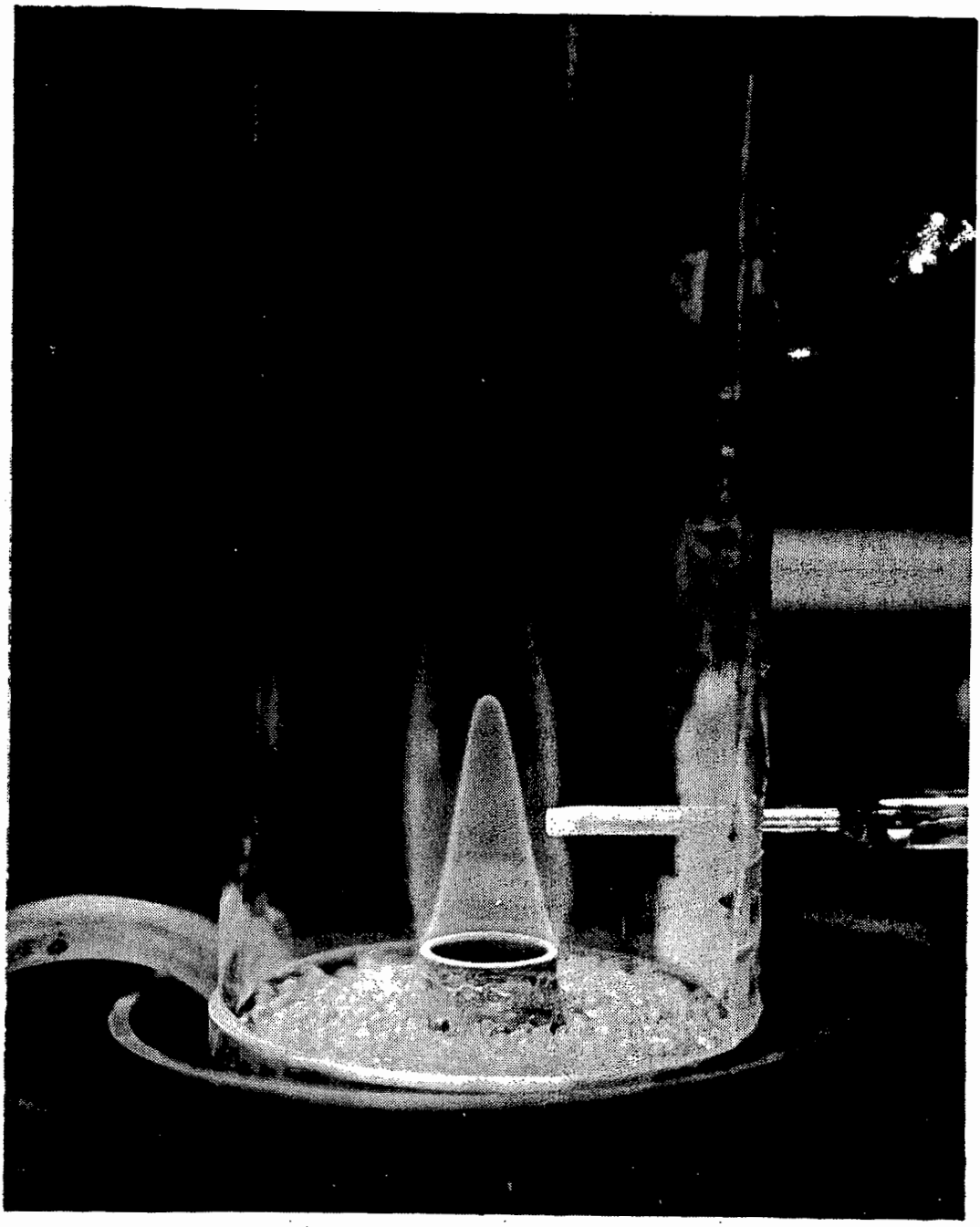

Figure 1.—QUARTZ PROBE AND 67% AERATED FLAME

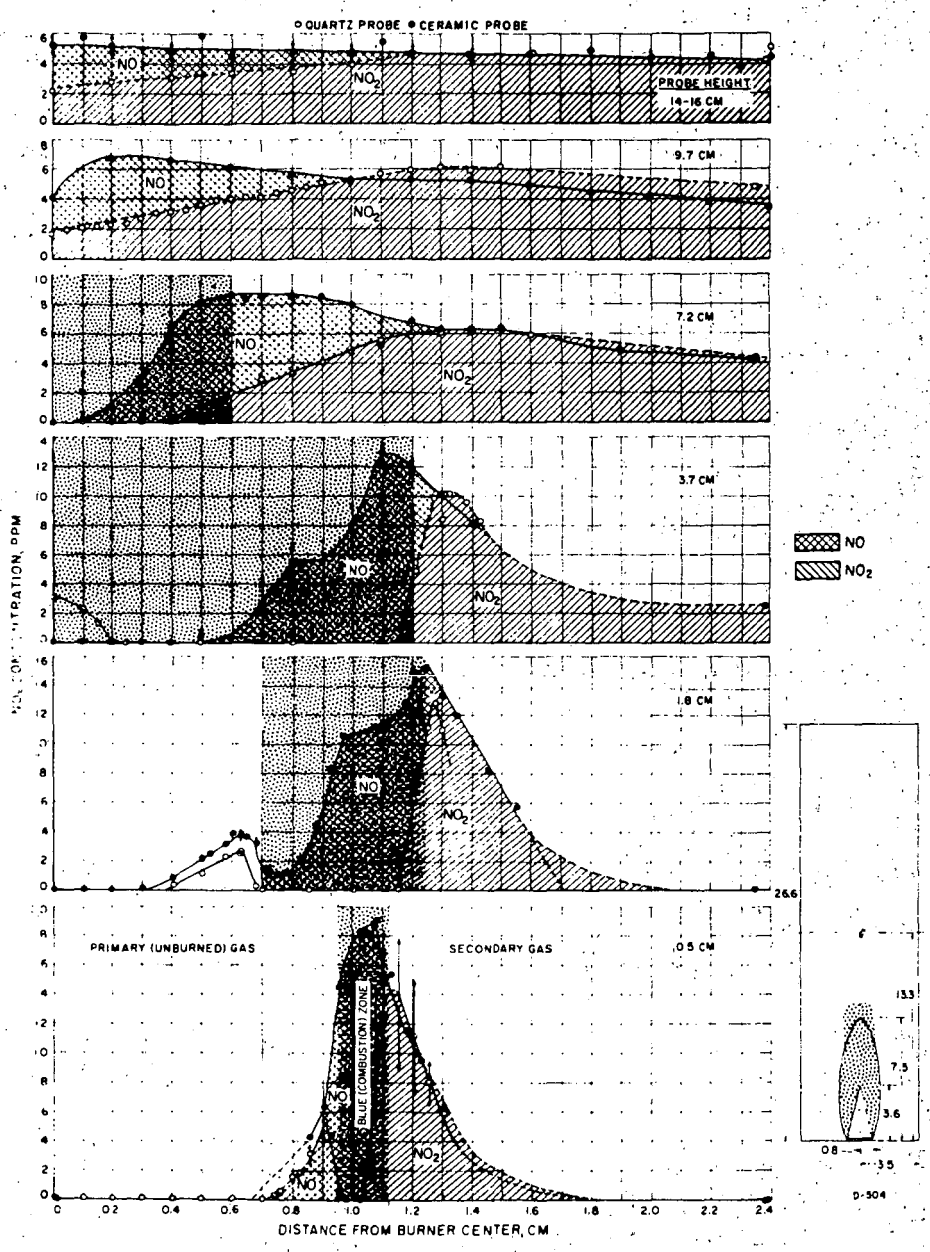

Figure 2.—NITROGEN OXIDE PROFILES AT VARIOUS HEIGHTS WITH 67% PRIMARY AERATED CONICAL FLAME

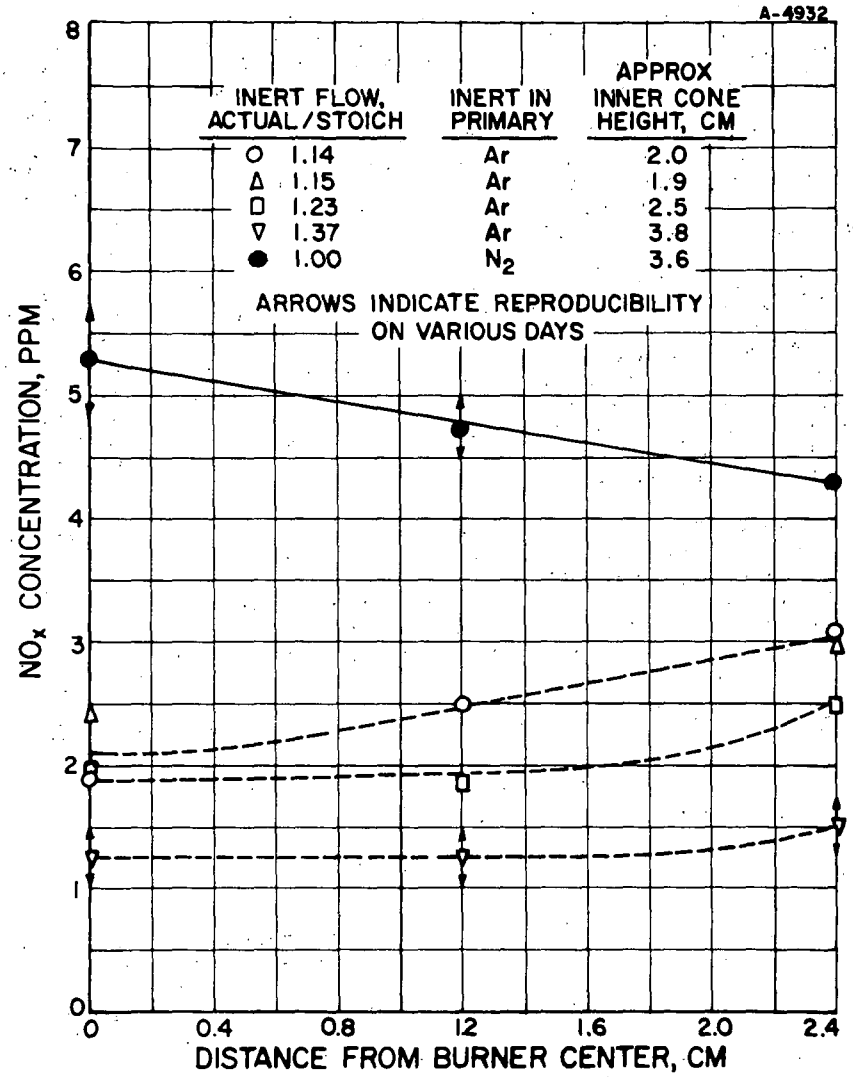

Figure 3.–CONCENTRATION OF NO_x 15 CENTIMETERS ABOVE THE FLAMEHOLDER OF A CONICAL CH_4-Ar-O_2 FLAME WITH 67% OF STOICHIOMETRIC O_2 IN THE PRIMARY STREAM

primary mixture flow rate has no apparent effect over the range of 12 to 20 CF/hr. There appears to be a small change in the concentration of NO_x as the input is increased to 25 CF/hr. The flow rate of the secondary stream has no effect over the same range.

The effect of primary aeration is not large over the range of 67 to 90 percent primary air. However, a strong decrease in the concentration of NO_x is observed when the primary mixture is made fuel-lean. Figure 4 shows the NO_x and NO_2 concentration profiles of a flame with 110 percent primary aeration. In contrast to the fuel-rich primary mixture (Figure 2), the primary oxide of nitrogen that is present is NO_2, rather than NO. The flame with the fuel-lean primary has only a single, small combustion zone as opposed to the two larger combustion zones with the fuel-rich primary. This may account for the decreased NO_x with the fuel-lean primary.

The shape and position of the reaction zone for the formation of NO_x from a bunsen or conical flame made a kinetic analysis difficult. Consequently, the experimental work was changed from a bunsen to a flat flame stabilized by a flameholder consisting of a collection of stainless steel capillary tubes. A more detailed series of data are being obtained with this burner.

One of the most interesting observations illustrated is in Figure 5, where the concentration of NO_2 along the centerline is shown as a function of height above the burner. The NO_2 is seen to form very close to the flame (which is at a height of about 0.1 cm), and then rapidly decompose. The NO_2 concentration decreases to zero with the fuel-rich and stoichiometric primary mixtures. However, some NO_2 is found at all heights above the burner with the fuel-lean primary mixtures. These data were obtained with nitrogen as the secondary gas. A similar effect is observed when argon is the secondary. However, the decomposition of NO_2 is greatly decreased when air is the secondary.

Figure 6 shows the effect of this decomposition on the relative concentrations of NO and NO_2 when an argon or air secondary is used with a primary mixture of 100.5 percent aeration. It is seen that there is more NO_2 present at a height of 1.1 cm with air than with argon. However, in either case, the primary oxide of nitrogen is NO near the burner centerline, but it is NO_2 near the secondary. Figure 7 shows that almost no NO is present at 0.1 cm above the burner. NO_2 is the primary oxide of nitrogen at all radial positions.

There are three significant observations to be drawn from this stoichiometric flame:

1) NO_2 is the oxide of nitrogen which is formed in the flame.
2) Some of this NO_2 decomposes to NO.
3) NO also forms by another mechanism in the combustion products above the flame.

These observations do not necessarily contradict the data from the bunsen flame, since there are a considerable number of differences between the two systems.

There are two regions of formation of NO_x by a flat flame. Figure 8 shows that NO_2 is formed from a methane-air primary steam with an argon secondary. This NO_2 which must have formed in the flame, is seen to decompose. Figure 9 shows that NO_2 is formed from a methane-argon-oxygen primary stream with an air secondary. This NO_2, which forms where the primary and secondary stream are mixing, does not appear to decompose to any significant extent. Temperature differences between these two regions may explain the different decompositions observed, since the same relative effect is noted when NO_2 is added to the primary mixture of a methane-argon-oxygen flame with an argon secondary. The decomposition is much greater near the center of the burner than near the secondary. We

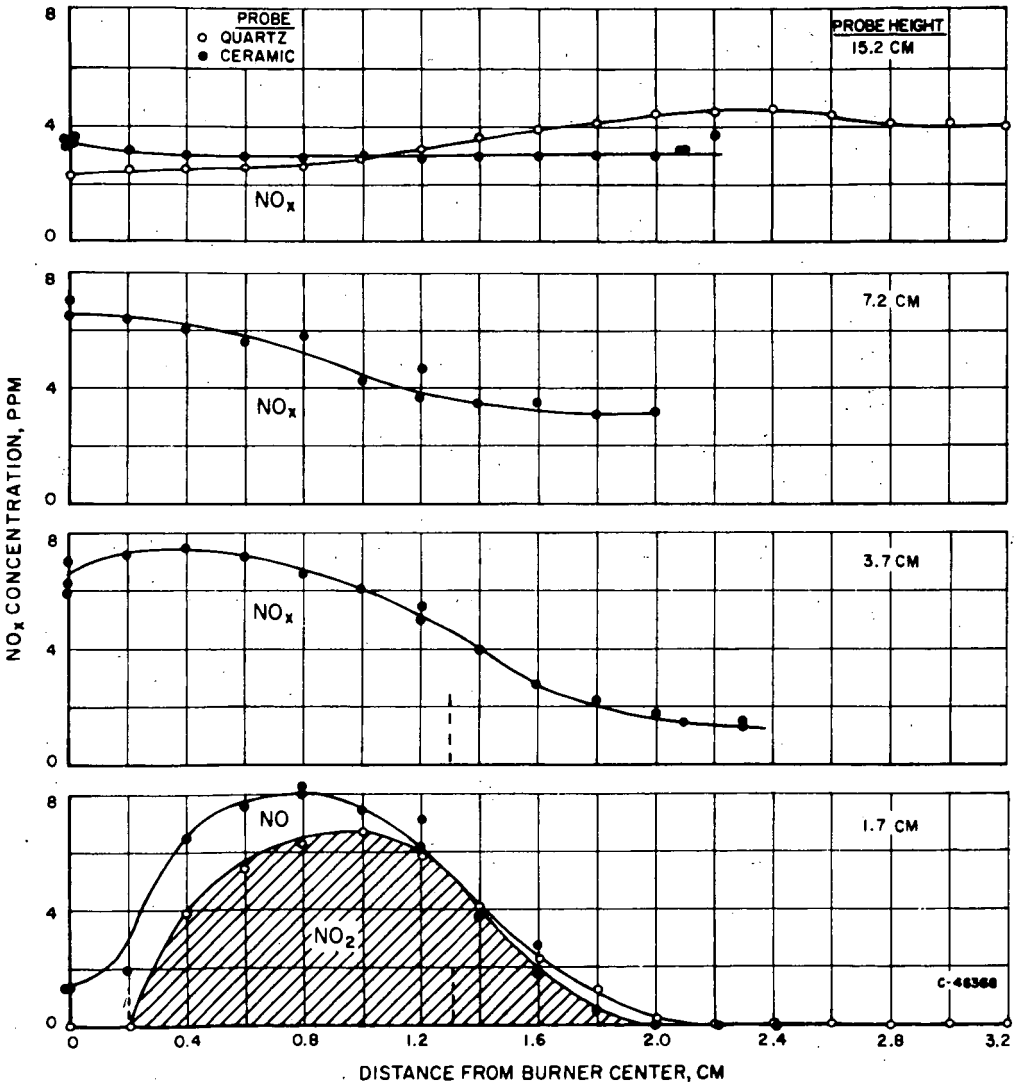

Figure 4.–NO_x CONCENTRATION PROFILES AT VARIOUS HEIGHTS WITH A 110% PRIMARY AERATED CONICAL FLAME

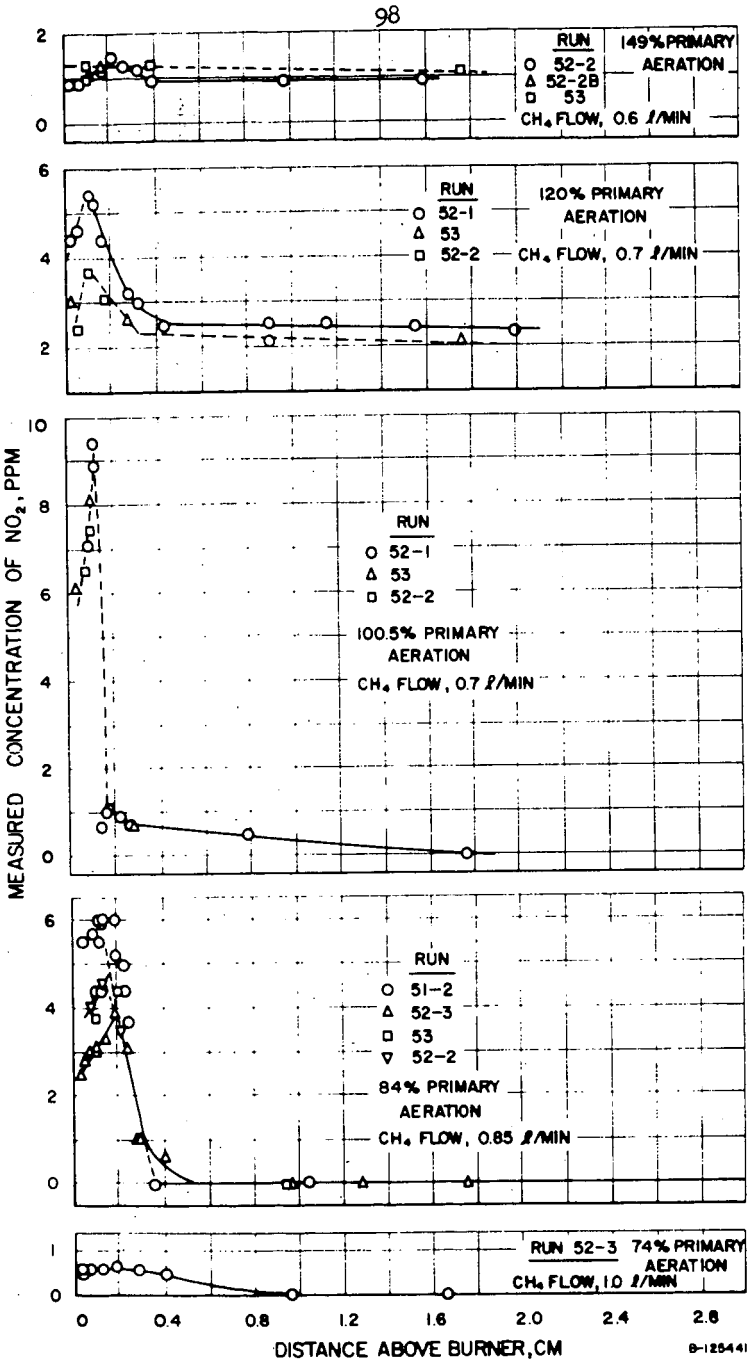

Figure 5.–AXIAL CENTERLINE CONCENTRATION PROFILES OF NO_2 FROM FLAT METHANE-AIR FLAMES WITH A SECONDARY NITROGEN ATMOSPHERE

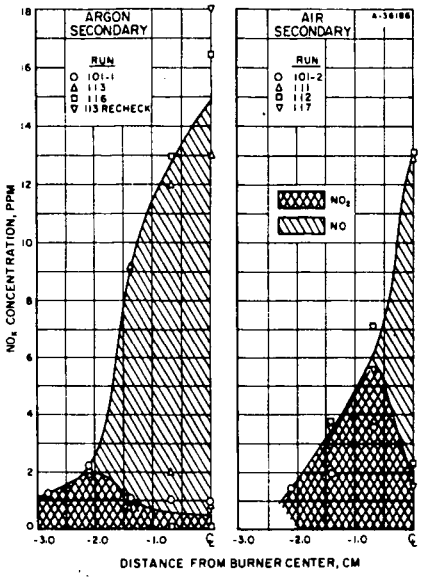

Figure 6.–NO_x CONCENTRATION FOR A CH_4-AIR STOICHIOMETRIC FLAME AT A HEIGHT OF 1.1 cm ABOVE THE BURNER

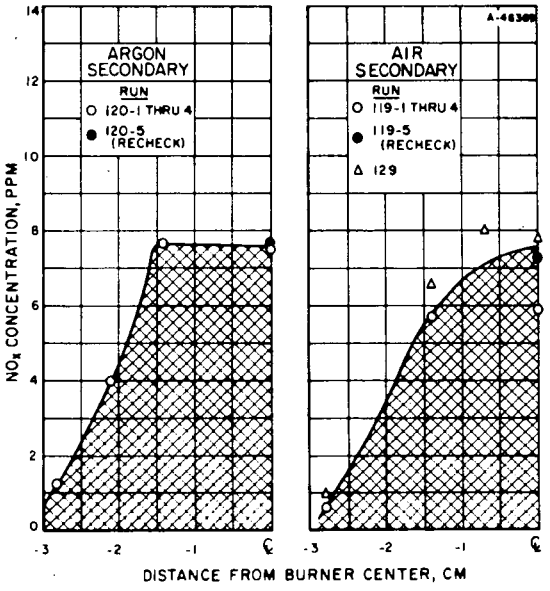

Figure 7.–NO_x CONCENTRATION FOR A CH_4-AIR STOICHIOMETRIC FLAME AT 0.1 cm ABOVE THE BURNER

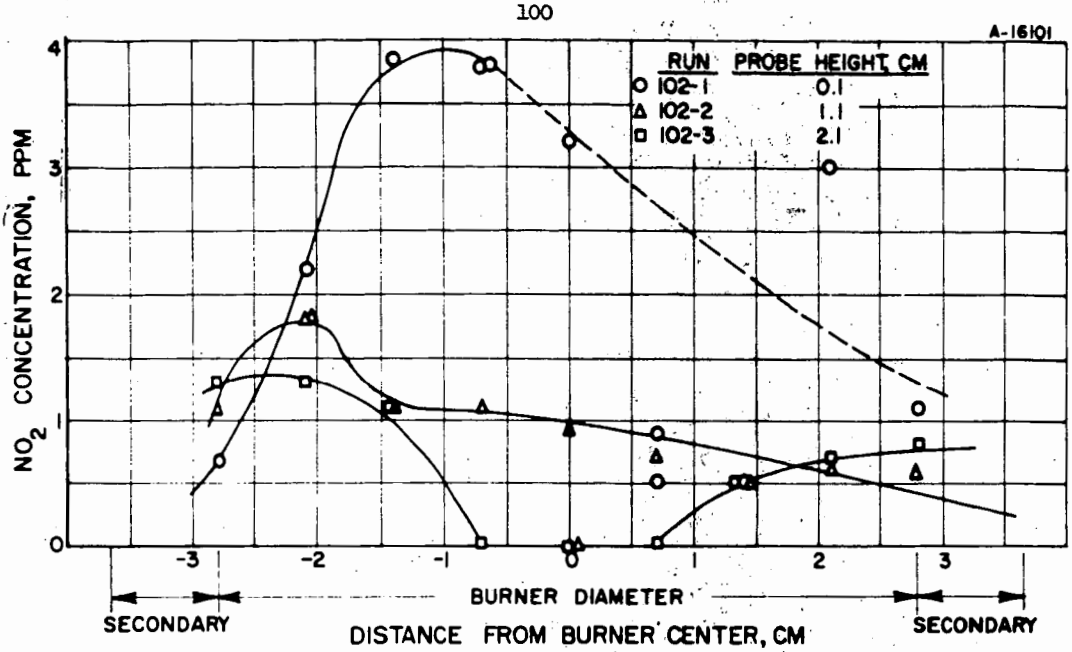

Figure 8.–FORMATION OF NO_2 FROM A STOICHIOMETRIC FLAT CH_4-AIR FLAME WITH A SECONDARY ARGON STREAM

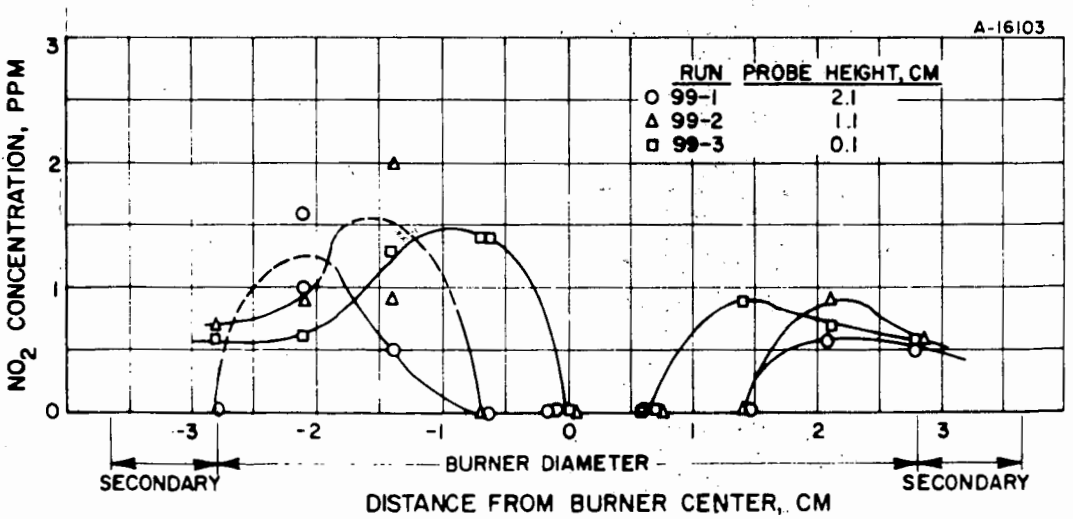

Figure 9.–FORMATION OF NO_2 FROM A STOICHIOMETRIC CH_4-Ar-O_2 FLAME WITH A SECONDARY AIR STREAM

are aware that there is some oxidation of NO to NO_2 in our sampling system. At present, the fraction oxidized appears to be small. We are interpreting the measured NO_2 as being primarily from the flame.

Theoretical equilibrium and kinetic studies are currently in process. Figure 10 shows the calculated concentration of NO_x in equilibrium[1] with the combustion products from flames of various compositions and various temperatures. At these temperatures, (above 1500°K), the ratio of the concentration of NO to that of NO_2 is more than 300:1. This ratio increases as the temperature increases or the oxygen concentration decreases.

The region where NO_x forms in the bunsen flame has relatively steep axial and radial temperature gradients. The estimated temperature range is from 2200° to 3100°R. The flat flame provides a radial region of more than 2.4 cm of very uniform temperature. The axial temperature gradient is only about 25°C/cm. The temperature above the flat flame has been estimated, with corrected thermocouple readings and published correlations,[2-4] to be about 1500° ± 100°C (2700°R).

Thus, there are no indications that total concentrations in excess of equilibrium are being formed from stoichiometric or fuel-lean flames. However, the ratio of NO to NO_2 is not characteristic of the high-temperature equilibrium. This may be due to the oxidation in the sampling system.

The kinetics of this system are extremely complex because of the flame reactions. However, it is possible to compare the values measured in this system with the amount of NO that would be formed in air heated to the same temperature for the same length of time. The kinetic model (in which M represents any other species) used for this calculation is:

$$N_2 + M \rightleftharpoons 2N + M$$
$$O_2 + M \rightleftharpoons 2O + M$$
$$N_2 + O \rightleftharpoons NO + N$$
$$O_2 + N \rightleftharpoons NO + O$$
$$N_2 + O_2 \rightleftharpoons 2NO$$

Table 4 gives the calculated rates at various temperatures. It is of interest to note that the rates of the bimolecular reaction and the atomic reactions to form NO are comparable at these temperatures. At higher temperatures, the atomic reactions will predominate.

Table 4.—RATES OF FORMATION OF NITRIC OXIDE IN AIR AT VARIOUS TEMPERATURES

Temperature, °K	Rate of Formation of Nitric Oxide, ppm/sec	
	NO = 100 ppm	NO = 10 ppm
1600	0.90	1.02
1800	69	73
2000	2150	2210

The time required for the combustion products to pass from 0.1 to 1.1 cm above the burner is about 0.026 second. During this time, the stoichiometric combustion products are observed to form a 10 ppm increase in NO_x.

If the same time factor is applied to the kinetics of heated air, the calculated concentrations are 1.8 ppm at 1800°K, and 57 ppm at 2000°K. It should be noted that:

1) The rate constants for this kinetic model are not well established, and the values

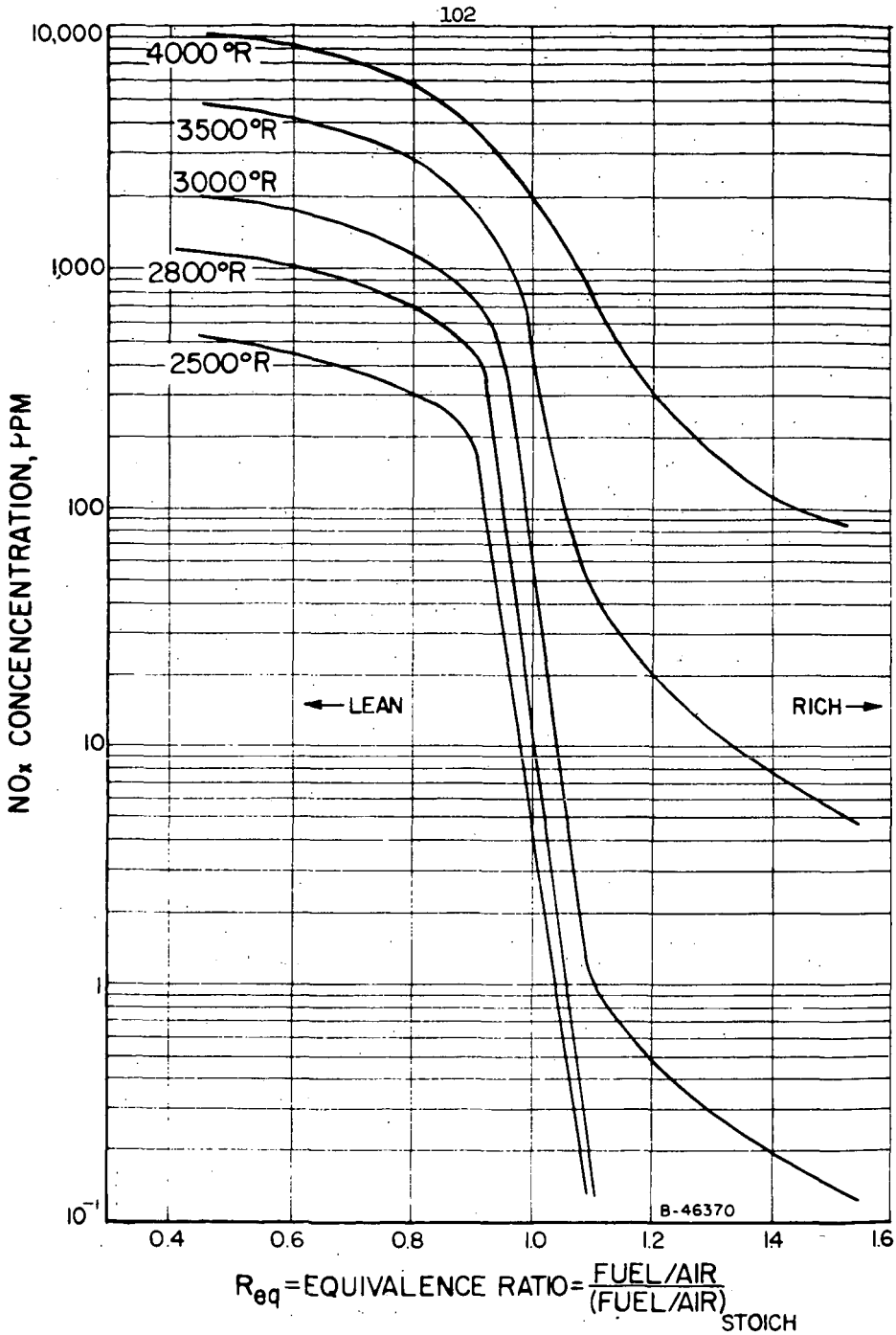

Figure 10.–EQUILIBRIUM OF NO_x WITH COMBUSTION PRODUCTS OF VARIOUS METHANE-AIR FLAMES

used in this calculation are among the highest that were found.[5]

2) The oxygen concentration of air is much larger than that of the stoichiometric combustion products by about 2 orders of magnitude.

3) The estimated temperature of the system is close to 1800 °K.

Thus, it appears likely that, upon completion of the theoretical analysis and with accurate temperature and composition measurements, it will be found that nitrogen oxides form in a flame faster than in heated air.

REFERENCES

1. Rossini, F. D., Pitzer, K. S., Arnett, R. L., Braun, R. M. and Pimental, G. C., "Selected Values of Physical and Thermodynamic Properties of Hydrocarbons and Related Compounds." Pittsburgh: Carnegie Press, 1953.

2. "Symposium on Gas Temperature Measurement," J. Inst. Fuel 12, S1-S108 (1939) March (Supplementary issue).

3. Weil, S. A., "Burning Velocities of Hydrocarbon Flames," Institute of Gas Technology Research Bulletin No. 30 (1961) March.

4. Weil, S. A., "A Study of Porous Plate Flameholders," Institute of Gas Technology Research Bulletin No. 35 (1964) August.

5. Wray, K. L., "Chemical Kinetics of High Temperature Air," Avco Research Rept. 104. Everett, Mass.: Avco-Everett Research Laboratory, 1961.

FLAME CHARACTERISTICS CAUSING AIR POLLUTION I. EMISSION OF OXIDES OF NITROGEN AND CARBON MONOXIDE

Joseph M. Singer
Edwin B. Cook
Joseph Grumer

U.S. Bureau of Mines, 4800 Forbes Avenue,
Pittsburgh, Pennsylvania

ABSTRACT

This investigation is part of a program by the Bureau of Mines, sponsored by the Public Health Service, to determine the factors that govern emission of air pollutants by domestic and industrial gas combustors. Methods based on kinetic and thermodynamic theory are proposed for predicting concentrations of nitrogen oxides and carbon monoxide in the combustion gases of flames, specifically of lean, stoichiometric, and rich propane-air flames. These theoretical data are compared with concentrations observed experimentally downstream of flat grid-type burner flames (approximately 25,000 Btu/hr) that were used to simulate gas appliances such as water and space heaters. Air pollutant concentrations were computed for (1) flames chemically perturbed by recycling flue gases into the primary fuel-air mixtures; (2) flames thermally perturbed by cooling the burned gases at different rates; and (3) flames perturbed by combinations of these two effects. In general, experimental and computed concentrations agreed to within a factor of 2 to 4 with the experimental values always being higher than the theoretical. Cooling the burned gases and recycling cold flue gases (with and without excess air) reduced the relative amount of nitric oxides. Carbon monoxide concentrations were substantially reduced by recycling flue gases only when the cooling rates were less than about 5000-10000°R per second.

TRACE ORGANIC COMPOUNDS IN NATURAL GAS COMBUSTION

by

J. A. Chisholm, Jr. and D. L. Klass

Institute of Gas Technology
Chicago, Illinois 60616

INTRODUCTION

Complete combustion is decidedly easier to obtain with natural gas than with any other fossil fuel.[5] Under normal operating conditions, the flue products of natural-gas-burning equipment are relatively free of unburned hydrocarbons and partial combustion products. However, under fuel-rich conditions, small quantities of organic derivatives are produced. The investigation reported in this paper to identify and determine the quantities of these trace compounds, particularly when combustion occurs under low-aeration conditions, was carried out at the Institute of Gas Technology, with financial support of the American Gas Association.

Classical wet chemical procedures lack the sensitivity and selectivity for analyses of these trace organic compounds. Consequently, highly sensitive instrumental methods were used, with modifications whenever necessary.

EQUIPMENT

The source of combustion products was the burner system shown in Fig. 1. It consists of a burner, transite base, and glass chimney. When the burner is operated at the low flow rates employed in this study, a bunsen-type flame is obtained. Disturbance of the flame by air currents, and dilution of the exhaust gases by surrounding air, were prevented by enclosing the burner in a pyrex glass chimney. Samples of flue products were withdrawn either from the top of the chimney or through the probe.

Early in the investigation, the base of the burner system was modified as shown in Fig. 2; a secondary air chamber, with 1/8-in. steel spheres in it to facilitate diffusion, was installed.

The burner was operated on 1000 Btu natural gas similar in composition to that shown in Table 1, and numerous experiments were carried out under a variety of conditions. Since space does not permit a detailed description of the experimental techniques, only a few comments can be made here.

Combustion conditions varied from fuel-rich to stoichiometric operation. The extreme fuel-rich variable corresponded to flow rates of 2 CF/hr of natural gas, no primary air, and 10 CF/hr of secondary air. Stoichiometric conditions corresponded to flow rates of 2 CF/hr of natural gas and 17.5 CF/hr of primary air. Secondary air was employed in selected stoichiometric experiments. Sufficient experiments were carried out to insure the reproducibility of the analytical determinations under the specific operating conditions. All determinations of specific

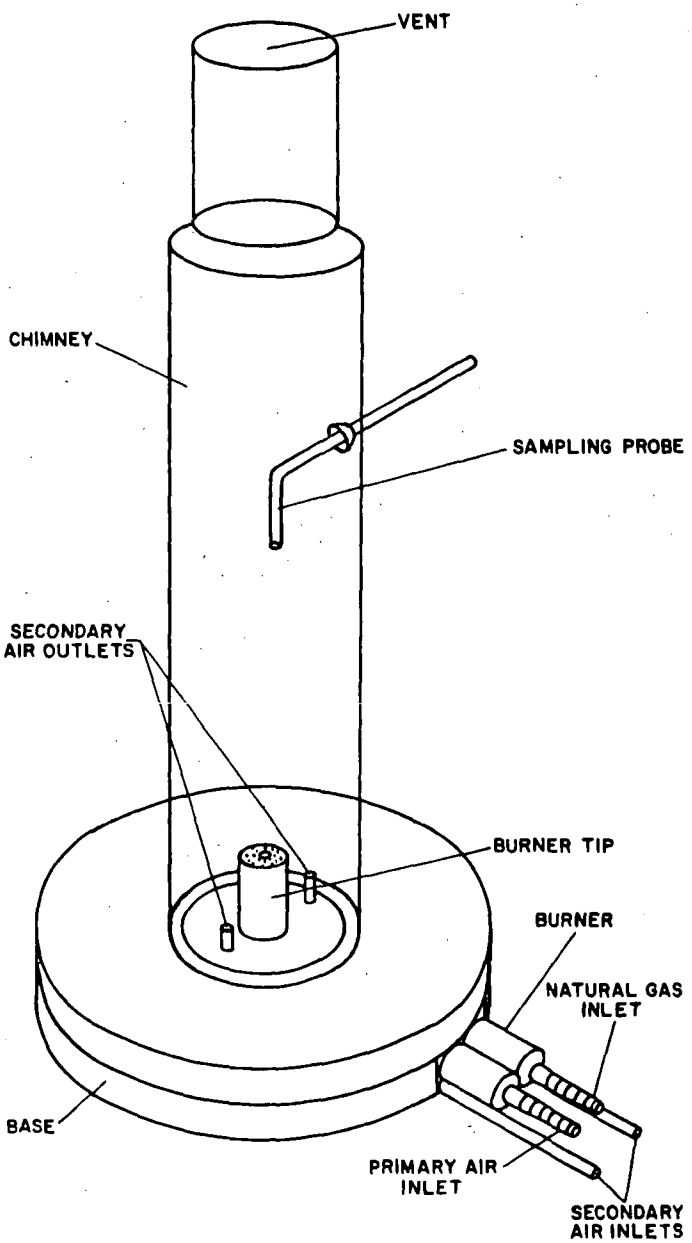

Fig. 1.-CLOSED BURNER SYSTEM FOR COMBUSTION OF NATURAL GAS

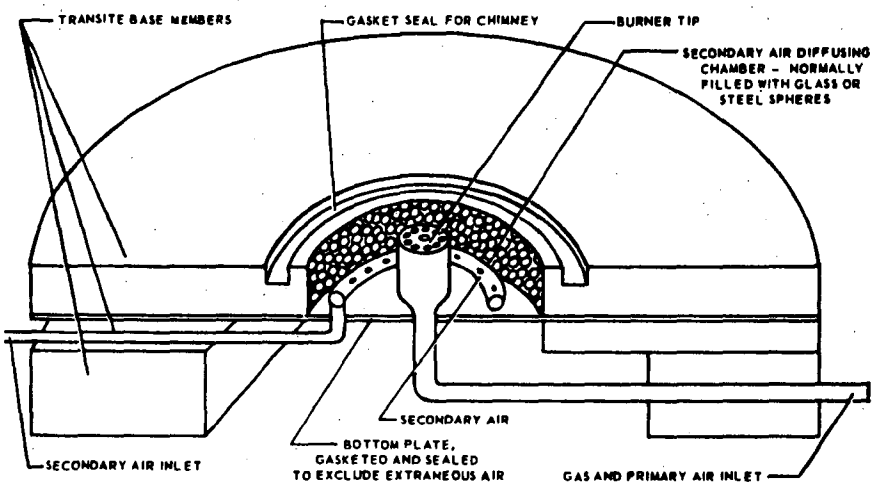

Fig. 2.—MODIFIED BURNER BASE

flue products were normalized to percentages of the total flue products.

RESULTS

During this investigation, a large number of saturated and unsaturated aliphatic, polynuclear aromatic, and oxygenated hydrocarbons were identified. Many were determined quantitatively in the ppb (parts per 10^9) concentration range. Table 2 gives a partial list of the organic compounds found in the combustion products under stoichiometric and fuel-rich operating conditions.

Gas chromatography with a flame ionization detector was employed to measure C_1 to C_5 saturated and unsaturated aliphatic hydrocarbons. Under essentially complete combustion conditions, the C_1 to C_3 hydrocarbons were present in the flue products in the ppb range, and several C_4 and C_5 compounds were below limits of detectability, as shown in Tables 3 and 4. When primary air was absent, concentrations of the C_1 to C_5 hydrocarbons varied inversely with the secondary air flow. Total C_5 + hydrocarbons were determined by reversing carrier gas flow in the chromatographic column and backflushing after the emergence of n-butane. Again, the inverse relationship of concentration to secondary air flow was observed, as shown in Table 5.

An alumina column operated at 80°C with argon carrier gas served to separate the C_1 to C_3 fraction. The C_4 to C_5 fraction was separated on a 1/8 in. x 15 ft column of 28% dimethylsulfolane on Chromasorb P. Separation of total C_5+ hydrocarbons was effected on a 1/8 in x 6 ft alumina column operating at 100°C.

Polynuclear aromatic hydrocarbons were collected in a low-temperature trapping system, and separated by means of liquid extraction procedures and column, paper, and gas chromatography. Ultraviolet absorption and fluorescence spectrophotometry were then employed to identify the separated fractions. By these techniques, fifteen polynuclear aromatic compounds were identified; seven of these were determined quantitatively. Quantitative determination was based on separation via column chromatography, and identification and measurement were accomplished by ultraviolet fluorescence spectrophotometry. Table 6 shows that the concentrations ranged from less than 0.1 ppb for o-phenylenepyrene under conditions of essentially complete combustion, to 1040 ppb for pyrene under fuel-rich conditions.

Several classes of oxygenated hydrocarbons were investigated, including aldehydes, phenols, and ketones. Because aldehydes are always produced during incomplete combustion,[18] these compounds were studied in some detail. The spectrophotometric methods used are specific for formaldehyde, acrolein, total aliphatic aldehydes and total aldehydes. Table shows that when only secondary air was present, the concentration of total aldehydes was inversely related to the flow of secondary air. In the absence of secondary air, but with sufficient primary air to ensure essentially complete combustion, aldehydes were produced in only ppb concentrations. Formaldehyde was predominant, and persisted under all but stoichiometric combustion conditions. With increased secondary air, a generally increasing ratio of formaldehyde to other aldehydes was observed. These findings are consistent with the reported stability of formaldehyde.[18]

Table 1.–Typical Analysis of Chicago Natural Gas

Component	Mole %	Component	Mole %
Air	3.21	Propane	1.21
Helium	0.08	n-Butane	0.17
Nitrogen	1.79*	i-Butane	0.08
Carbon dioxide	0.63	Pentanes	0.04
Methane	88.21	Hexanes	0.03
Ethane	4.51	Heptanes	0.04
			100.00

Heating Value - 1001 Btu/SCF, Saturated gas at 60°F, 30 in. Hg.
*Nitrogen in excess of that included in air.

Table 2.–TYPES AND QUANTITIES OF ORGANIC COMPOUNDS FOUND IN THE COMBUSTION PRODUCTS OF A NATURAL GAS FLAME

Type of Compound	Concentration Found after Stoichiometric Combustion	Concentration Found after Fuel-Rich Combustion
Aldehydes:		
Formaldehyde	< 0.02 ppm	20 ppm
Other Aliphatic Aldehydes	< 0.02	13
Nonaliphatic Aldehydes	< 0.02	6
Total Aldehydes	< 0.02	39
Polynuclear Aromatics:		
Anthanthrene	< 3.0 ppb	275 ppb
Anthracene	< 0.4	46
Benzo [a] pyrene	0.4	89
Fluoranthene	6.0	468
1-Methylpyrene	0.6	78
o-Phenylenepyrene	0.1	84
Pyrene	14.0	1040
Other Hydrocarbons:		
Methane	0.08 ppm	60,000 ppm
Ethane	0.13	3,500
Propane	0.10	900
i-Butane	< 0.01	50
n-Butane	< 0.01	70
Pentane plus	< 5.00	120
Acetylene	< 0.01	2,500
Ethylene	0.06	4,000
Propylene	< 0.01	260

Table 3.–CONCENTRATION OF SOME C_1 - C_4 HYDROCARBONS AT VARIOUS AERATION LEVELS

Air Input, CF/hr		Concentration ppm							
		Alkanes					Alkenes		
Primary	Secondary	Methane	Ethane	Propane	i-Butane	n-Butane	Ethylene	Propylene	Acetylene
0	30	0.08*	-	0.02	< 0.01	< 0.01	0.09	< 0.01	< 0.01
		0.08*	-	0.11	< 0.01	< 0.01	0.03	< 0.01	< 0.01
0	25	3.4	0.16	0.11	< 0.01	< 0.01	0.84	0.07	4.6
		1.6	0.09	0.04	< 0.01	< 0.01	0.61	< 0.02	3.3
		5.2	0.16	0.01	< 0.01	< 0.01	1.37	0.03	4.7
0	20	2800	23.3	0.17	< 0.02	< 0.02	161	2.3	240
		2100	25.0	0.13	< 0.02	< 0.02	162	2.1	240
		1900	22.1	0.16	< 0.02	< 0.02	182	2.1	250
0	17.5	7000	72	1.3	< 0.02	< 0.02	410	7.8	910
		7300	72	1.3	< 0.02	< 0.02	470	7.7	850
		7300	69	1.3	< 0.02	< 0.02	470	7.9	880
0	15	12,500	117	2.3	0.06	0.06	910	17.5	1400
		16,300	138	2.2	0.05	0.04	1080	20.2	1500
		14,600	-	2.5	0.8	0.06	1030	20.1	1500
0	12.5	26,200	343	7.0	-	0.25	1700	68.0	1900
		29,200	352	6.9	0.04	0.17	1800	58.5	2000
		29,000	441	6.2	0.13	0.20	1800	57.5	2000
0	10	58,300	1223	45.4	2.2	3.8	3700	118	2600
		39,100	964	42.1	1.5	2.2	3100	108	2600
		33,200	1048	48.7	0.6	3.9	2700	97	2300
20	0	0.04*	-	< 0.01	< 0.01	< 0.01	< 0.01	< 0.01	< 0.01
		0.04*	-	< 0.01	< 0.01	< 0.01	< 0.01	< 0.01	< 0.01
		0.04*	-	< 0.01	< 0.01	< 0.01	< 0.01	< 0.01	< 0.01
15	0	0.41*	-	< 0.01	< 0.01	< 0.01	< 0.01	< 0.01	< 0.01
		0.37*	-	< 0.01	< 0.01	< 0.01	< 0.01	< 0.01	< 0.01
		0.44*	-	< 0.01	< 0.01	< 0.01	< 0.01	< 0.01	< 0.01
12.5	0	12.8*	-	< 0.01	< 0.01	< 0.01	1.5	< 0.01	5.2
		5.4*	-	< 0.01	< 0.01	< 0.01	.5	< 0.01	2.4
		15.4*	-	< 0.01	< 0.01	< 0.01	2.4	< 0.01	9.2
		19.2*	-	< 0.01	< 0.01	< 0.01	3.2	< 0.01	-
10	10	.05*	-	< 0.01	< 0.01	< 0.01	< 0.01	< 0.01	< 0.01
		.05*	-	< 0.01	< 0.01	< 0.01	< 0.01	< 0.01	< 0.01

* Composite methane and ethane peak.

Table 4. — AIR FLOW VS. C_4-C_5 CONCENTRATIONS

Run No.	41b	40a	40b	41a	42a
Flow Rates, CF/hr					
Primary Air	0	0	0	0	17.5
Secondary Air	10	15	20	25	0
Natural Gas	2	2	2	2	2
Concentration, ppm*					
Butene-1	1820	550	165	17	<0.05
i-Butene	<0.05	<0.05	<0.05	<0.05	<0.05
trans-Butene-2	50	8	2	<0.05	<0.05
i-Pentane	<0.05	<0.05	<0.05	<0.05	<0.05
cis-Butene-2	<0.05	<0.05	<0.05	<0.05	<0.05
Pentane	<0.05	<0.05	<0.05	<0.05	<0.05
3-Methylbutene-1	<0.05	<0.05	<0.05	<0.05	<0.05
1,3-Butadiene	40	9	1	<0.05	<0.05
Pentene-1	118	43	7	<0.05	<0.05

* Chromatograph calibrated on basis of response to n-butane

Table 5.—C_5 + HYDROCARBONS

*Air Input, CF/hr, Primary	Secondary	Total C_5+ Hydrocarbons, ppm	Air Input, CF/hr Primary	Secondary	Total C_5+ Hydrocarbons, ppm
5	10	<5	0	25	<5
5	5	30	0	20	<5
			0	15	<5
			0	12.5	80
2.5	10	<5	0	12.5	100
2.5	7.5	20	0	10	90
2.5	7.5	14	0	7.5	110
2.5	5	85	0	7.5	144

* Natural Gas Input, 1 CF/hr

Table 6.–POLYNUCLEAR AROMATIC HYDROCARBONS DETERMINED IN NATURAL GAS COMBUSTION PRODUCTS

	Flow Rate, CF/hr — Run No.				
Aeration Conditions	9	5R	7	8	10
Primary air	0	0	0	0	17.5
Secondary air	10	15	20	25	0
Natural gas	2	2	2	2	2
Component	Concentration, ppb				
Anthanthrene	240	275	11	<3	<3
Anthracene	26	46	6	6	<0.4
Benzo[a]pyrene	89	78	40	11	0.4
Fluoranthene	434	468	256	117	6
1-Methylpyrene	78	48	11	4	0.6
o-Phenylenepyrene	75	75	84	43	<0.1
Pyrene	1040	454	155	103	14

Table 7.–AIR FLOW VS. ALDEHYDE PRODUCTION

Run No.	Flow Rates, CF/hr			Aldehyde Concentration, ppm		
	Primary Air	Secondary Air	Natural Gas	Formaldehyde	Aliphatic Aldehydes	Total Aldehydes
3	0	10	2	19.4	32.9	39.3
4	0	15	2	18.4	25.6	34.6
5	0	20	2	13.4	13.1	18.5
6	0	25	2	2.4	1.9	6.0
8	17.5	0	2	<0.02	<0.01	<0.02

The unsaturated aldehyde acrolein occurs in the exhaust gases from most combustion processes.[2,7,8,12] Under fuel-rich combustion conditions, acrolein concentrations ranging from less than 0.03 ppm (parts per million) to about 6 ppm (Table 8) were determined by a spectrophotometric method.

Phenols are another group of oxygenated organic derivatives that is known to be present in combustion products from natural gas flames.[13] Total phenol concentrations varied from 0.007 ppm to about 4 ppm (Table 9).

Several spectrophotometric procedures were investigated for determination of ketones, but interference from water and formaldehyde introduced excessive error. Gas chromatography, however, resulted in accurate determinations of several ketones, as shown in Table 10.

Chromatographic studies gave tentative evidence of the presence of methyl and ethyl alcohols in the flue products. Quantitative measurements were not made, but methyl alcohol peak areas indicated concentrations of about 3 ppm.

DISCUSSION

The experimental data collected in our investigation of the flue products from fuel-rich flames might be interpreted in terms of numerous hypothetical reaction mechanisms that have no real meaning. Instead, let us consider how the formation of trace components produced under poor combustion conditions can be rationalized and qualitatively explained in terms of a few reaction mechanisms which are known to be operative in fuel-rich flames. (Carbenes and perhaps methyne are very likely involved in the formation of flue-gas combustion products, but they are not considered in this treatment.)

Many of the major mechanisms operative in lean flames are reasonably well understood, but the organic chemistry of fuel-rich flames presents a considerably more complex situation.[3] The initial reactions in a fuel-rich methane-oxygen flame have been shown to involve formation of methyl radicals, which are probably produced by hydrogen atom abstraction:[3]

$$CH_4 + H \rightarrow CH_3 + H_2$$

The methyl radicals might be called the "key intermediates" in the combustion of methane in fuel-rich systems because their concentration is sufficient to produce other structures by conversion to higher molecular weight intermediates. Subsequent chemical reactions of methyl radicals in fuel-rich flames therefore determine, to a large extent, the structures of the partial combustion products. We should thus be able to relate our experimental results to these methyl radical reactions, especially those that occur with small or essentially zero activation energies.

First, the reaction of methyl radicals with oxygen would not be expected to be the dominant one in an oxygen-deficient flame, but the reaction should occur to some degree with formation of peroxy radicals:

$$CH_3 + O_2 \rightarrow CH_3OO \rightarrow H-\overset{O}{\overset{\|}{C}}-H + OH$$

Table 8.-AIR FLOW VS. ACROLEIN PRODUCTION

Run	Natural Gas, CF/hr	Air, CF/hr		Acrolein, ppm
		Primary	Secondary	
21	2	17.5	0	<0.03
22	2	0	10	6.3
23	2	0	15	5.6
24	2	0	20	5.3
25	2	0	25	2.9

Table 9. -AIR FLOW VS. PHENOL PRODUCTION

Run No.	Flow Rates, CF/hr			Phenol Concentration, ppm*
	Primary Air	Secondary Air	Natural Gas	
4	0	10	2	4.0
5	0	15	2	4.1
6	0	20	2	1.0
7	0	25	2	0.5
8	17.5	0	2	0.026
9	25.0	0	2	0.007

*Calibration curves were prepared with phenol solutions as standards.

Table 10.-AIR FLOW VS. CARBONYL PRODUCTION

Run	Natural Gas, CF/hr	Air, CF/hr		Carbonyl Production, ppm			
		Primary	Secondary	Acetaldehyde	Acrolein-Acetone	Propionaldehyde	2-Butanone
363-1	2	0	10	6.2	1.5	0.07	1.6
363-2	2	0	15	3.4	0.8	0.03	1.0
363-3	2	0	20	2.9	1.2	0.05	1.8
363-4	2	0	25	5.0	1.5	0.01	2.8

These radicals are known to decompose rapidly to yield formaldehyde.[14,17] Further oxidation of formaldehyde would be expected, even in an oxygen-deficient flame, because of the high reactivity of aldehyde groups.

Since the rate of formation of formaldehyde should be greater than the rates of formation of the higher aldehydes from the methyl-radical-derived intermediates that will be discussed later, we would expect formaldehyde to be present in higher concentrations than the other aldehydes in the flue gases. As already shown in Tables 2 and 7, over half of the total aldehydes in almost all of our experiments was formaldehyde when the flue products were produced under oxygen-deficient conditions.

Recombination of excess methyl radicals in oxygen-deficient flames:

$$2CH_3 \rightarrow CH_3CH_3$$

would be favored over methyl radical-oxygen reactions, so larger concentrations of ethane relative to formaldehyde would be expected in the flue gases. The formation of ethane in this type of recombination reaction, however, is not as simple as it appears. When the new carbon-to-carbon bond is formed, a large amount of energy is liberated. This energy, along with the original thermal energy carried by the methyl radicals, can dissociate ethane back to methyl radicals, or the resulting vibrationally excited ethane molecules can be deactivated by a three-body collision process. In the presence of a third body, such as another molecule with which the energy-rich ethane molecules collide, the excess energy can be transferred with concurrent formation of substantial amounts of ethane without homolytic dissociation to methyl radicals. However, according to Kistiakowsky,[4] the energy-rich ethane molecules initially produced do not necessarily require a three-body process to prevent dissociation.

Since methyl radical recombination is a direct one-step path to a stable paraffin, one would expect larger concentrations of ethane than the higher paraffins in the flue gases. This conclusion is supported by the results summarized in Table 2. Significantly higher concentrations of ethane than propane were detected in the flue products under oxygen-deficient conditions. The concentrations of propane were in turn higher than the total C_4+ paraffin concentrations. The natural gases studied in this investigation contained a few percent ethane and propane, but the relative ratios of these hydrocarbons in the flue gases should still be indicative of the combustion mechanism.

The mechanism of formation of ethylene and acetylene in a methane-rich flame has not been fully established, but the general course of the reactions is believed to proceed through C_2 radical intermediates.[11] Successive dehydrogenation of ethane yields ethylene and acetylene. The detailed mechanism of the dehydrogenation is not known.[9] Homolytic C-H bond rupture by unimolecular decomposition or hydrogen atom abstraction should be facilitated in methane-rich flames, because methyl radical recombination affords energy-rich ethane molecules. We therefore expect that stepwise dehydrogenation of ethane proceeds via an ethyl radical intermediate:

$$CH_3CH_3 \rightarrow CH_3CH_2 + H$$

to yield substantial amounts of ethylene and acetylene relative to the

other unsaturates. Formation of ethyl radicals subsequently provides direct routes to propane and the butanes, but dehydrogenation should be the preferred reaction path because of the favorable kinetics at high temperatures.[9]

Thus, the formation and relative concentration of the major oxygenated and saturated and unsaturated aliphatic compounds detected as trace components in the flue gases of methane-rich flames have been rationalized on the basis of a few known radical reactions. It should be emphasized that these reactions are by no means the only paths to the observed compounds, but their relationship to the experimental results indicates that they are important.

It is much more difficult to explain the formation of the polynuclear aromatics listed in Table 2. Grossly empirical reaction mechanisms must be postulated because of the complexity of polynuclear aromatic structures.[15] Nevertheless, we believe that a few important conclusions can be drawn from the data collected in our work.

Most investigators who have studied the formation of polynuclear aromatics found that these compounds generally form under fuel-rich conditions.[6,15] Our data, which include determinations of both aliphatic and aromatic compounds, show that fuel-rich conditions promote polynuclear aromatics formation, but at very low levels relative to the concentrations of the aliphatic compounds. It is therefore difficult to select a particular aliphatic compound, or group of compounds, as key intermediates in the mechanism of formation of the aromatic compounds.

Aliphatic intermediates are, however, clearly the precursors of the aromatic compounds because the natural gases used in our experiments contained zero polynuclear aromatics. Various investigators have suggested that methyne and unsaturates such as ethylene and acetylene play an important role as intermediates.[6,10,11,15] Empirical reaction paths have also been postulated to account for the formation of polynuclear aromatics from these and other intermediates.[15]

In several experiments, our determinations of the polynuclear aromatics formed in fuel-rich flames tend to fall into a particular pattern. The higher molecular weight polynuclear aromatics in the flue gas were consistently present in lower concentrations than those of lower molecular weight. Although other investigators have reported similar results,[10] this information is insufficient for valid conclusions regarding the mechanisms of formation.

However, significant observations can be made. The distribution of the aromatics was about the same in each of our experiments, as shown in Table 6. Furthermore, this distribution corresponds essentially to that reported by others.[6,10,15] Finally, we observed that the relative concentrations of a few specific polynuclear aromatics are consistently higher than the concentrations of the other aromatics.

These observations suggest that the overall scheme shown in Fig. 3 is a plausible route to the various aromatic compounds identified in our studies. The reactive species and fragments involved in the many reactions required to produce the polynuclear aromatics are, of course, not known. But our results and their apparent relationship to the scheme in Fig. 3 support a stepwise buildup of the higher aromatics through common intermediates. A similar scheme can also be developed with Lindsey's data.[10]

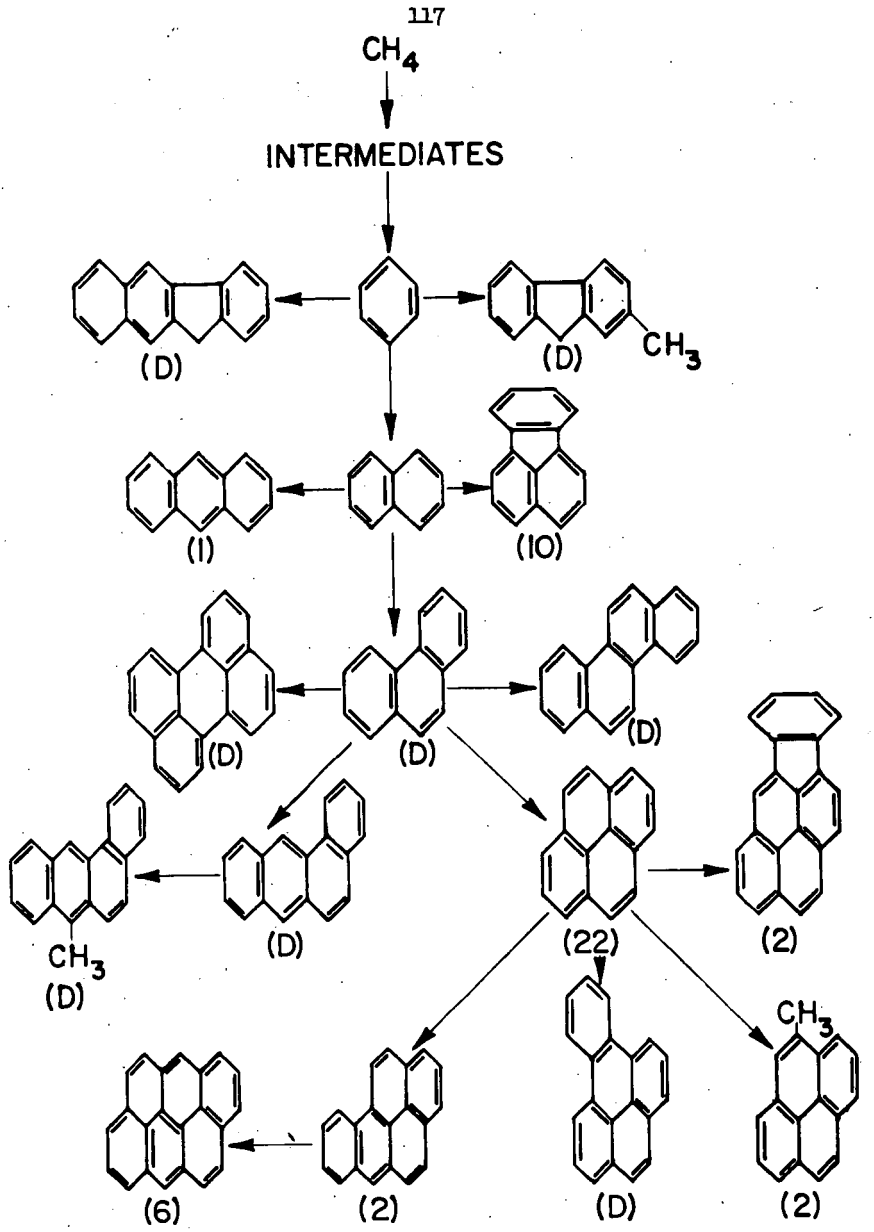

Fig. 3.—POSSIBLE ROUTES TO POLYNUCLEAR AROMATIC COMPOUNDS

Other interpretations of the distribution of the aromatics (Table 2), such as consideration of their relative stabilities, can be employed to rationalize the results. For example, linearly annellated acenes are known to be more reactive than phenes containing the same number of rings.[1] Thus, one would not expect a large concentration of acenes relative to the angularly annellated phenes in the flue products. Our experimental data show that only one acene, anthracene, was detected. Most of the polynuclear aromatics determined in this investigation contain the phenanthrene nucleus.

Quantitative treatment of the distribution of polynuclear aromatics in terms of electron densities and bond localization energies will be attempted when additional data have been compiled.

REFERENCES CITED

1. Clar, E. J., "Polycyclic Hydrocarbons," Vol. 1. New York: Academic Press, 1964.

2. Cohen, I. R. and Altshuller, A. P., "A New Spectrophotometric Method for the Determination of Acrolein in Combustion Gases and in the Atmosphere," Anal. Chem. 33, 726-33 (1961) May.

3. Fristrom, R. M. and Westenberg, A. A., "Flame Structure," Chapter XIV. New York: McGraw-Hill Book Company, 1965.

4. Gomer, R. and Kistiakowsky, G. B. The Rate Constant of Ethane Formation From Methyl Radicals," J. Chem. Phys. 19, 85-91 (1951) January.

5. Griswold, S. S., Chass, R. L., George, R. E. and Holmes, R. G., "An Evaluation of Natural Gas as a Means of Reducing Industrial Air Pollution," J. Air Pollution Control Assoc. 12, 155-63 (1962) April.

6. Hangebrauck, R. P., Von Lehmden, D. J. and Meeker, J. E., "Emissions of Polynuclear Hydrocarbons and Other Pollutants From Heat-Generation and Incineration Processes," J. Air Pollution Control Assoc. 14, 267-78 (1964) July.

7. Hughes, K. J. and Hurn, R. W., "A Preliminary Survey of Hydrocarbon-Derived Oxygenated Material in Automobile Exhaust Gases," J. Air Pollution Control Assoc. 10, 367-73 (1960) October.

8. Kryacos, G., Menapace, H. R. and Boord, C. E., "Gas-Liquid Chromatographic Analysis of Some Oxygenated Products of Cool-Flame Combustion," Anal. Chem. 31, 222-25 (1959) February.

9. Leroux, P. J. and Mathieu, P. M., "Kinetics of the Pyrolysis of Methane to Acetylene," Chem. Eng. Progr. 59, 54-59 (1961) November.

10. Lindsey, A. J., "The Formation of Polycyclic Aromatic Hydrocarbons and Carbon Deposits From Normal and Reversed Diffusion Flames," Combust. Flame 4, 261-64 (1960) September.

11. Miller, S. A. "Acetylene; Its Properties, Manufacture, and Uses," Vol. 1. New York: Academic Press, 1965.

12. Sharma, R. K., McLean, D. R. and Bardwell, J., "An Apparatus for the Analysis of Combustion Products Obtained during the Oxidation of Hydrocarbons, "Indian J. Technol. 3, 206-08 (1965) July.

13. Smith, R. G., MacEwen, J. D. and Barrow, R. E., "The Occurrence of Phenols in Air and Combustion Products," Am. Ind. Hyg. Assoc. J. 20 149-52 (1959).

14. Sugden, T. M., "Reactions of Free Radicals in the Gas Phase," Special Publication No. 9. London: The Chemical Society, 1957.

15. Tebbens, B. D., Thomas, J. F. and Mukai, M., "Hydrocarbon Synthesis in Combustion," A.M.A. Arch. Ind. Health 13, 567-73 (1956) June; ibid, "Aromatic Hydrocarbon Production Related to Incomplete Combustion," A.M.A. Arch. Ind. Health 14, 413-25 (1956) November.

16. Thomas, J. F., Sanborn, E. N., Mukai, M. and Tebbens, B. D., "Aldehyde Production Related to Combustion and Polluted Atmospheres," Ind. Eng. Chem. 51, 774-75 (1959) January.

17. Walsh, A. D., "Processes in the Oxidation of Hydrocarbon Fuels - II.," Trans. Faraday Soc. 43, 297-305 (1947).

18. Wilson, K. W., "Fixation of Atmospheric Carbonyl Compounds by Sodium Bisulfite," Anal. Chem. 30, 1127-29 (1958) June.